SIAM J. IMAGING SCIENCES
Vol. 15, No. 2, pp. 860–891

Imaging Anisotropic Conductivities from Current Densities*

Huan Liu†, Bangti Jin‡, and Xiliang Lu§

Abstract. In this paper, we propose and analyze a reconstruction algorithm for imaging an anisotropic conductivity tensor in a second-order elliptic PDE with a nonzero Dirichlet boundary condition from internal current densities. It is based on a regularized output least-squares formulation with the standard $L^2(\Omega)^{d,d}$ penalty, which is then discretized by the standard Galerkin finite element method. We establish the continuity and differentiability of the forward map with respect to the conductivity tensor in the $L^p(\Omega)^{d,d}$-norms, the existence of minimizers and optimality systems of the regularized formulation using the concept of H-convergence. Further, we provide a detailed analysis of the discretized problem, especially the convergence of the discrete approximations with respect to the mesh size, using the discrete counterpart of H-convergence. In addition, we develop a projected Newton algorithm for solving the first-order optimality system. We present extensive two-dimensional numerical examples to show the efficiency of the proposed method.

Key words. anisotropic conductivity, current density, Tikhonov regularization, H-convergence, Hd-convergence, projected Newton method

AMS subject classifications. 35R25, 35R30, 47J06

DOI. 10.1137/21M1437810

1. Introduction.

The conductivity value varies widely with soft tissue types [21, 40] and its imaging can provide valuable information about the physiological and pathological conditions of tissue [5]. This underpins several important medical imaging modalities [10, 3, 52, 49, 53, 4, 1]. For example, electrical impedance tomography (EIT) [10, 52] aims at recovering the interior conductivity distribution from boundary voltage measurement. However, it is severely ill-posed, and the attainable resolution is limited, and the uniqueness for anisotropic conductivity is only for a given conformal class [16, 31] (see [23] for some numerics). To overcome the ill-posed nature in EIT, MREIT (magnetic resonance EIT) employs an MRI scanner to capture the internal magnetic flux density data $\vec{b}$ induced by an externally injected current [30, 47, 27, 22] and then obtains the current density $\vec{h}$ according to Ampere's law $\vec{h} = \mu_0^{-1}\nabla \times \vec{b}$, where μ_0 is the magnetic permeability of free space. This requires

*Received by the editors August 2, 2021; accepted for publication (in revised form) March 2, 2022; published electronically June 23, 2022.
https://doi.org/10.1137/21M1437810
Funding: The work of the first author was partially supported by the National Natural Science Foundation of China grant 12101276 and the Ph.D. research startup foundation of Jinling Institute of Technology, grants 040521200103 and jit-fhxm-202117. The work of the second author was supported by EPSRC grant EP/T000864/1. The work of the third author was supported by National Key Research and Development Program of China grant 2020YFA0714200 and National Science Foundation of China grant 11871385.

†College of Science, Jinling Institute of Technology, Nanjing 211169, People's Republic of China (huanliumath@jit.edu.cn).
‡Department of Computer Science, University College London, London, WC1E 6BT, UK (b.jin@ucl.ac.uk).
§School of Mathematics and Statistics, Wuhan University, and Hubei Key Laboratory of Computational Science (Wuhan University), Wuhan 430072, People's Republic of China (xllv.math@whu.edu.cn).

measuring all components of the magnetic flux $\vec{b}$, which may be challenging in practice, as it requires a rotation of the domain being imaged or of the MRI scanner.

The use of internal data promises much improved resolution, and the reconstruction problem has received much attention. Kwon, Lee, and Yoon [34] proposed a noniterative reconstruction method for recovering an isotropic conductivity using equipotential lines, and proved the unique recovery from one current density vector $\vec{h}$ in two dimensions. Later, an iterative algorithm known as J-substitution was proposed [35]. With the knowledge of the magnitude of only one current density magnitude $|\vec{h}|$, the problem was studied in [42, 43, 54] in the isotropic case and in the anisotropic case in a known conformal class in [25]. Ammari et al. [6] studied the recovery of an anisotropic conductivity proportional to a known conductivity tensor.

It is widely accepted that most biological tissues have anisotropic conductivity values. The ratio of the anisotropy depends on the type of tissue and human skeletal muscle shows anisotropy of up to 10 between the longitudinal and transversal directions [46]. The conductivity for cell membrane, muscle fiber, or nerve fiber structure must be investigated using an anisotropic tensor model [44, 45, 5]. It arises naturally also in the mathematical modeling of boundary deformation [2]. Therefore, there has been a growing interest in recovering anisotropic conductivities [48, 8, 7, 37, 38, 39]. The potential of using current densities to recover anisotropic conductivity A was studied in [48]. The uniqueness of recovering an anisotropic resistivity distribution from current densities has been established [8, 7] (see also [37, 38] for power densities and [39] for three-dimensional numerical implementation). Bal, Guo, and Monard [8] showed that a minimum number of current densities ensures a unique and explicit reconstruction of the conductivity tensor A locally, and that the reconstruction of A is about the loss of one derivative compared to errors in the measurement of $\vec{h}$. Ko and Kim [32] gave a resistive network-based reconstruction method for three sets of internal electrical current densities, by directly discretizing Faraday's law. In addition, Hsiao and Sprekels [26] investigated the stability of recovering matrices of the form $A = \nabla p \otimes \nabla u$.

In this work, we consider the inverse problem of recovering an anisotropic conductivity tensor $A(x)$ from internal current densities $\vec{h} = A\nabla u$, where $u \in H^1(\Omega)$ solves

$$\begin{cases} -\operatorname{div}(A\nabla u) = f & \text{in } \Omega, \\ u = g & \text{on } \Gamma, \end{cases} \tag{1.1}$$

where $\Omega \subset \mathbb{R}^d$ $(d = 2, 3)$ is an open bounded Lipschitz domain with a boundary Γ, and $(f, g) \in (H^1(\Omega))' \times H^{\frac{1}{2}}(\Gamma)$. The anisotropic conductivity tensor $A(x) = (A_{ij}(x))_{i,j=1}^d$ belongs to the following admissible set:

$$\mathcal{A} = \left\{ A \in L^\infty(\Omega)^{d,d} : A(x) \in \mathcal{S}_d, \alpha|\xi|^2 \le \sum_{i,j=1}^d A_{ij}(x)\xi_i\xi_j \le \beta|\xi|^2 \quad \forall \xi \in \mathbb{R}^d \text{ a.e. } x \in \Omega \right\} \tag{1.2}$$

with constants $0 < \alpha < \beta < +\infty$, where $\mathcal{S}_d$ denotes the set of all $d \times d$ symmetric matrices endowed with the Frobenius inner product. We use the notation $u(A)(f, g)$ to explicitly

indicate the dependence of the solution u on the conductivity A. The $L^p(\Omega)^{d,d}$-norm ($1 \le p < \infty$) on $\mathcal{A}$ is given by

$$\|\!|A|\!\|_p = \Big(\int_\Omega \sum_{i,j=1}^d |A_{i,j}(x)|^p dx \Big)^{\frac{1}{p}},$$

and for the case $p = \infty$, it is defined in terms of supremum as usual. When $p = 2$, it is naturally induced by an inner product, which is denoted by $(\cdot,\cdot)_{L^2(\Omega)^{d,d}}$ below. For the recovery of the conductivity tensor A, suppose that we are given a set of L measurements $\vec{h}^\ell$, $\ell = 1, \ldots, L$, corresponding to the excitations (f^ℓ, g^ℓ), $\ell = 1, \ldots, L$. To handle the ill-posedness of the inverse problem, we consider the standard Tikhonov regularization [17, 28], i.e., the least-squares data fitting regularized with an $L^2(\Omega)^{d,d}$ penalty. More precisely, given the regularization parameter $\gamma > 0$, we minimize the following regularized functional over the admissible set $\mathcal{A}$:

$$\min_{A\in\mathcal{A}} \Big\{ J_\gamma(A) = \frac{1}{2} \sum_{\ell=1}^L \|A\nabla u^\ell(A)(f^\ell, g^\ell) - \vec{h}^\ell\|^2_{L^2(\Omega)^d} + \frac{\gamma}{2} \|\!|A|\!\|_2^2 \Big\}. \tag{1.3}$$

Note that the formulation (1.3) involves only the $L^2(\Omega)^{d,d}$ penalty, and it is suitable for recovering both smooth and discontinuous conductivity tensors. However, the choice of the $L^2(\Omega)^{d,d}$ penalty introduces certain challenges in the mathematical and numerical analysis of the regularized problem, due to a lack of weak sequential closeness of the parameter-to-state map. One way to address this issue is to use a stronger norm for the penalty, e.g., $\|\cdot\|_{H^1(\Omega)}$, but it can be numerically cumbersome to treat the ellipticity constraint (i.e., the bounds on the extremal eigenvalues of the tensor A in the admissible set $\mathcal{A}$; cf. (1.2)).

In this work, we provide a detailed analysis of the reconstruction approach, e.g., the parameter-to-state map, especially $L^p(\Omega)^{d,d}$ differentiability, well-posedness of the variational formulation (1.3) (existence of a minimizer, optimality system and consistency), and the finite element discretization and its convergence. One distinct challenge in the analysis arises from the fact that the regularized formulation (1.3) involves only an $L^2(\Omega)^{d,d}$ penalty, which does not induce strong compactness. In order to resolve the challenge, we resort to the concept of H-convergence [51, 41] and its discrete analogue, i.e., Hd-convergence [19] (developed for a finite volume scheme). In order to apply the concept, the presence of a nonzero Dirichlet boundary condition in the governing model (1.1) necessitates revisiting known H-convergence results; see Theorems 2.8 and 3.3 for the precise statements. Further, we present extensive numerical results to validate the approach, and the numerical results show clearly the efficiency and accuracy of the approach.

Numerical algorithms for recovering matrix parameters have not been extensively studied [33, 14, 15]. Kohn and Lowe [33] introduced a variational method involving a convex functional for recovering a matrix-valued diffusion coefficient but did not present numerical experiments. Deckelnick and Hinze [14, 15] studied the identification of matrix parameters in elliptic PDEs from measurements $(z, f) \in Z \times H^{-1}(\Omega)$ ($Z = L^2(\Omega)$ or $Z = H_0^1(\Omega)$) using the concept of H-convergence. This work is inspired by [14, 15]. However, there are major differences between these works and this work. First, the model in [14, 15] has a zero Dirichlet boundary

condition, but the model (1.1) involves a nonzero Dirichlet boundary condition. The presence of a nonzero Dirichlet boundary condition, inherent to the concerned inverse problem, poses big challenges to the mathematical and numerical analysis of the regularized formulation (1.3). Most studies deal only with a zero Dirichlet boundary condition, and the concept of H-convergence and its discrete analogue (i.e., Hd-convergence) have to be revisited, which in particular requires establishing relevant fundamental results; cf. Theorems 2.8 and 3.3 for the continuous and discrete H-convergence results with a nonzero Dirichlet boundary condition, respectively. This represents the major technical novelty of the study. Second, in [15], the authors carry out the optimization by the projected steepest descent method with Armijo's rule, whereas we solve the resulting optimization problem by a Newton type algorithm from measurements $(A\nabla u, g) \in L^2(\Omega)^d \times H^{\frac{1}{2}}(\Gamma)$, which is numerically observed to be highly efficient and accurate, when coupled with a path-following strategy. Third, we give a detailed analysis of the continuity and differentiability of parameter-to-state map, which is essential for rigorously developing the numerical algorithm (see also the work [54] for relevant results). Last, the works [14, 15] are concerned with variational discretization of the conductivity tensor, which greatly facilitates the convergence analysis, whereas this work analyzes the Hd-convergence for general discretization of the conductivity tensor A.

The rest of the paper is organized as follows. In section 2, we analyze the well-posedness of the formulation (1.3), including existence, optimality system, and consistency, using the concept of H-convergence. Then in section 3, we develop the finite element discretization, prove the convergence of the approximations as the mesh size h tends to zero using the concept of Hd-convergence, and describe a projected Newton method for solving the smoothed optimality system. Last, in section 4, we present several two-dimensional examples to illustrate distinct features of the proposed approach. Throughout, the notation C denotes a generic constant, which may differ at different occurrences but does not depend on the matrix A and any functions/parameters (e.g., mesh size h) involved in the analysis. The notation $(\cdot,\cdot)$ with suitable subscripts denotes the $L^2(\Omega)$, $L^2(\Omega)^d$, or $L^2(\Omega)^{d,d}$ inner product, and $\langle\cdot,\cdot\rangle$ denotes the duality pairing, e.g., between $H_0^1(\Omega)$ and its dual $H^{-1}(\Omega)$.

2. The regularized formulation.

In this section, we study the well-posedness of the regularized formulation (1.3) using the concept of H-convergence.

2.1. Preliminary estimates.

For any fixed $(f,g) \in (H^1(\Omega))' \times H^{\frac{1}{2}}(\Gamma)$, and any $A \in \mathcal{A}$, problem (1.1) has a unique solution $u \in H^1(\Omega)$. The parameter-to-state map $F : A \mapsto u$ is defined by $u = F(A)(f,g)$. We often write $u = F(A)$, by suppressing the dependence on the problem data (f,g). By the Lax–Milgram theorem, we have the following a priori regularity estimate of the solution u to problem (1.1).

Lemma 2.1. *For any $A \in \mathcal{A}$ and $(f,g) \in (H^1(\Omega))' \times H^{\frac{1}{2}}(\Gamma)$, there exists a unique solution $u = F(A) \in H^1(\Omega)$ to problem (1.1), and it satisfies*

$$\|u\|_{H^1(\Omega)} \le C(\|f\|_{(H^1(\Omega))'} + \|g\|_{H^{\frac{1}{2}}(\Gamma)}).$$

Lemma 2.1 implies that $u \equiv F(A)$ is uniformly bounded in $H^1(\Omega)$ for any fixed $(f,g) \in (H^1(\Omega))' \times H^{\frac{1}{2}}(\Gamma)$. Actually, the regularity can be slightly improved using Meyers' gradient

estimates [36, Theorem 1]. We denote by $Q := Q(\alpha, \beta) \in (2, \infty)$, defined in [36, Theorem 1], by suppressing its dependence on d, which satisfies $Q \to 2$ as $\frac{\alpha}{\beta} \to 0$ and $Q \to r$ (r is given in Theorem 2.2) as $\frac{\alpha}{\beta} \to 1$. The next result gives an $L^q(\Omega)$ gradient estimate for a nonzero Dirichlet boundary condition. Throughout, let

$$Q_d = \begin{cases} \min(Q, 4), & d = 2, \\ \min(Q, 3), & d = 3. \end{cases}$$

Theorem 2.2. *Let $\Omega \subset \mathbb{R}^d (d = 2, 3)$ be a bounded C^r domain, with $r \in (2, \infty)$, and $A \in \mathcal{A}$. For any $f \in L^2(\Omega)$ and $g \in H^1(\Gamma)$, let $u \in H^1(\Omega)$ be a weak solution of problem (1.1). Then, for any $2 < q < Q_d$, problem (1.1) has a unique solution $u \in W^{1,q}(\Omega)$, and there exists $C = C(\alpha, \beta, d, q, \Omega) > 0$ such that*

$$\|u\|_{W^{1,q}(\Omega)} \le C(\|f\|_{L^2(\Omega)} + \|g\|_{H^1(\Gamma)}).$$

Proof. Let $\bar{u}$ be the solution to the Laplace equation $-\triangle \bar{u} = 0$ in Ω with $\bar{u}|_\Gamma = g \in H^1(\Gamma)$. Then by the standard elliptic regularity theory, we obtain $\bar{u} \in H^{\frac{3}{2}}(\Omega)$, and $\|\nabla \bar{u}\|_{H^{\frac{1}{2}}(\Omega)} \le C\|g\|_{H^1(\Gamma)}$. For any $q \in Q_d$, by the Sobolev embedding theorem [18],

$$H^{\frac{1}{2}}(\Omega) \hookrightarrow \begin{cases} L^4(\Omega), & d = 2 \\ L^3(\Omega), & d = 3 \end{cases} \hookrightarrow L^q(\Omega). \tag{2.1}$$

Thus,

$$\|\nabla \bar{u}\|_{L^q(\Omega)} \le C\|\nabla \bar{u}\|_{H^{\frac{1}{2}}(\Omega)} \le C\|g\|_{H^1(\Gamma)}.$$

Let $w := u - \bar{u} \in H_0^1(\Omega)$, which satisfies

$$\begin{cases} -\mathrm{div}(A\nabla w) = \mathrm{div}(A\nabla \bar{u}) + f & \text{in } \Omega, \\ w = 0 & \text{on } \Gamma. \end{cases}$$

By Meyers' gradient estimate for a zero Dirichlet boundary problem [36, Theorem 1], we have

$$\|\nabla w\|_{L^q(\Omega)^d} \le C(\|A\nabla \bar{u}\|_{L^q(\Omega)^d} + \|f\|_{L^2(\Omega)}) \le C(\|A\|_{L^\infty(\Omega)^{d,d}} \|\nabla \bar{u}\|_{L^q(\Omega)^d} + \|f\|_{L^2(\Omega)}).$$

This and the triangle inequality complete the proof of the theorem. ∎

The following Hölder inequality for matrix- and vector-valued functions is useful.

Lemma 2.3. *If $\frac{1}{p} + \frac{1}{q} = \frac{1}{2}$, $p, q \ge 1$, then for $A \in L^p(\Omega)^{d,d}$, $u \in W^{1,p}(\Omega)$, and $v \in H^1(\Omega)$, there holds*

$$|(A\nabla u \cdot \nabla v)_{L^2(\Omega)^d}| \le d^{\frac{1}{2}+\frac{1}{q}} |||A|||_p \|\nabla u\|_{L^q(\Omega)^d} \|\nabla v\|_{L^2(\Omega)^d}. \tag{2.2}$$

Proof. By the Cauchy–Schwarz inequality and Hölder inequality with conjugate exponents satisfying $\frac{1}{m} + \frac{1}{n} = 1$, we have

$$
\begin{aligned}
&|(A\nabla u\cdot\nabla v)_{L^2(\Omega)^d}|\\
&\le \|A\nabla u\|_{L^2(\Omega)^d}\|\nabla v\|_{L^2(\Omega)^d} = \Big(\int_\Omega \sum_{i=1}^d (\sum_{j=1}^d A_{ij}\partial_j u)^2 dx\Big)^{\frac12}\|\nabla v\|_{L^2(\Omega)^d}\\
&\le \Big(\int_\Omega \sum_{i=1}^d (\sum_{j=1}^d |A_{ij}|^m)^{\frac{2}{m}} (\sum_{j=1}^d |\partial_j u|^n)^{\frac{2}{n}} dx\Big)^{\frac12}\|\nabla v\|_{L^2(\Omega)^d}\\
&\le \Big(\int_\Omega (\sum_{i=1}^d (\sum_{j=1}^d |A_{ij}|^m)^{\frac{2}{m}})^m dx\Big)^{\frac{1}{2m}} \Big(\int_\Omega (\sum_{j=1}^d |\partial_j u|^n)^2 dx\Big)^{\frac{1}{2n}}\|\nabla v\|_{L^2(\Omega)^d}\\
&\le \Big(\int_\Omega d^{m-1}(\sum_{i=1}^d (\sum_{j=1}^d |A_{ij}|^m)^2) dx\Big)^{\frac{1}{2m}} \Big(\int_\Omega d(\sum_{j=1}^d |\partial_j u|^{2n}) dx\Big)^{\frac{1}{2n}}\|\nabla v\|_{L^2(\Omega)^d}\\
&\le \Big(\int_\Omega d^m(\sum_{i,j=1}^d |A_{ij}|^{2m}) dx\Big)^{\frac{1}{2m}} d^{\frac{1}{2n}} \Big(\int_\Omega \sum_{j=1}^d |\partial_j u|^{2n} dx\Big)^{\frac{1}{2n}}\|\nabla v\|_{L^2(\Omega)^d}\\
&= d^{\frac12+\frac{1}{2n}} \Big(\int_\Omega \sum_{i,j=1}^d |A_{ij}|^{2m} dx\Big)^{\frac{1}{2m}} \Big(\int_\Omega \sum_{j=1}^d |\partial_j u|^{2n} dx\Big)^{\frac{1}{2n}}\|\nabla v\|_{L^2(\Omega)^d}.
\end{aligned}
$$

Upon taking $q = 2n$ and $p = 2m$, the desired inequality follows. ∎

Now we can derive the Lipschitz continuity of the parameter-to-state map $F(A)$ with respect to the $|||\cdot|||_p$ -norm for any $p \in (\frac{2Q_d}{Q_d-2}, \infty]$.

Lemma 2.4. *For any $f \in L^2(\Omega)$ and $g \in H^1(\Gamma)$, the mapping $F : A \mapsto u(A)$ is Lipschitz continuous from $(\mathcal{A}, L^p(\Omega)^{d\times d})$ to $H^1(\Omega)$ for any $p \in (\frac{2Q_d}{Q_d-2}, \infty]$. That is, for any $A_1, A_2 \in \mathcal{A}$,*

$$\|F(A_2) - F(A_1)\|_{H^1(\Omega)} \le C(\alpha,\beta,d,p,\Omega)(\|f\|_{L^2(\Omega)} + \|g\|_{H^1(\Gamma)})|||A_2 - A_1|||_p.$$

Proof. Let $u_1 = F(A_1)$ and $u_2 = F(A_2)$ be the weak solutions to problem (1.1) with A_1 and A_2, respectively. By the weak formulations, we deduce

$$(A_1(\nabla u_2 - \nabla u_1), \nabla v)_{L^2(\Omega)^d} = -((A_2 - A_1)\nabla u_2, \nabla v)_{L^2(\Omega)^d} \quad \forall v \in H_0^1(\Omega). \tag{2.3}$$

Take $q \in (2, Q_d)$ such that $\frac1p + \frac1q + \frac12 = 1$, and let $v = u_2 - u_1 \in H_0^1(\Omega)$ in (2.3). Then the definition of $\mathcal{A}$ and Lemma 2.3 imply

$$\alpha\|\nabla(u_2 - u_1)\|^2_{L^2(\Omega)^d} \le d^{\frac12+\frac1q}|||A_2 - A_1|||_p\|\nabla u_2\|_{L^q(\Omega)^d}\|\nabla(u_2 - u_1)\|_{L^2(\Omega)^d}.$$

By Theorem 2.2, there exists a constant $C = C(\alpha,\beta,d,q,\Omega)$ such that

$$\|u_2 - u_1\|_{H^1(\Omega)} \le C|||A_2 - A_1|||_p(\|f\|_{L^2(\Omega)} + \|g\|_{H^1(\Gamma)}),$$

which directly gives the desired assertion. ∎

Next we show the directional differentiability of the map F. Fix $A \in \mathcal{A}$, and let $H \in L^\infty(\Omega)^{d,d}$ be a feasible direction such that $A + tH \in \mathcal{A}$ for small $t > 0$. Let $w \in H_0^1(\Omega)$ be the weak solution to the linearized problem

$$\begin{cases} \operatorname{div}(A\nabla w) = -\operatorname{div}(H\nabla u) & \text{in } \Omega, \\ w = 0 & \text{on } \Gamma. \end{cases} \tag{2.4}$$

This allows defining a linear map $DF(A) : L^p(\Omega)^{d,d} \mapsto H_0^1(\Omega)$ by $DF(A)[H] = w$. Now we show that the map $DF(A)$ is bounded and represents the derivative of F with respect to A in a generalized sense.

Proposition 2.5. *Let $f \in L^2(\Omega)$ and $g \in H^1(\Omega)$. Then for any $p \in (\frac{2Q_d}{Q_d-2}, \infty]$, the operator $DF(A) : L^p(\Omega)^{d,d} \mapsto H_0^1(\Omega)$ is bounded:*

$$\|w\|_{H^1(\Omega)} \le C(\alpha, \beta, d, p, \Omega)|||H|||_p(\|f\|_{L^2(\Omega)} + \|g\|_{H^1(\Gamma)}).$$

Further, for any $p \in (\frac{4Q_d}{Q_d-2}, \infty]$, the map $F(A)$ is differentiable in the sense that for any $A, A + H \in \mathcal{A}$, there holds

$$\lim_{|||H|||_p \to 0} \frac{\|F(A+H) - F(A) - DF(A)[H]\|_{H^1(\Omega)}}{|||H|||_p} = 0. \tag{2.5}$$

Proof. Fix $H \in L^\infty(\Omega)^{d,d}$, $f \in L^2(\Omega)$, and $g \in H^1(\Gamma)$. The weak formulation of problem (2.4) is to find $w \in H_0^1(\Omega)$ such that

$$(A\nabla w, \nabla v)_{L^2(\Omega)^d} = -(H\nabla u, \nabla v)_{L^2(\Omega)^d} \quad \forall v \in H_0^1(\Omega).$$

Choose $q \in (2, Q_d)$ such that $\frac{1}{p} + \frac{1}{q} + \frac{1}{2} = 1$. Then Lemma 2.3 and letting $v = w \in H_0^1(\Omega)$ give

$$\alpha\|\nabla w\|_{L^2(\Omega)^d}^2 \le d^{\frac{1}{2}+\frac{1}{q}}|||H|||_p\|\nabla u\|_{L^q(\Omega)^d}\|\nabla w\|_{L^2(\Omega)^d}.$$

By Theorem 2.2, there exists a constant $C = C(\alpha, \beta, d, q, \Omega)$ such that

$$\|DF(A)[H]\|_{H^1(\Omega)} \le C|||H|||_p(\|f\|_{L^2(\Omega)} + \|g\|_{H^1(\Gamma)}).$$

This shows the first assertion. Let $R = F(A + H) - F(A) - DF(A)[H]$. Then R satisfies

$$\begin{cases} \operatorname{div}((A+H)\nabla R) = -\operatorname{div}(H\nabla w) & \text{in } \Omega, \\ R = 0 & \text{on } \Gamma. \end{cases}$$

With $\frac{1}{p} + \frac{1}{q} = \frac{1}{2}$, the preceding argument leads to $\|\nabla R\|_{L^2(\Omega)^d} \le C|||H|||_p\|w\|_{L^q(\Omega)^d}$. Since w satisfies (2.4), by [36, Theorem 1], we deduce

$$\|\nabla w\|_{L^q(\Omega)^d} \le C\|H\nabla u\|_{L^q(\Omega)^d}.$$

The choice of $p \in (\frac{4Q_d}{Q_d-2}, \infty]$ implies $q \in (2, \frac{4Q_d}{2+Q_d}) \subset (2, Q_d)$. By choosing $\varepsilon > 0$ such that $\bar{q} = q + \varepsilon = \frac{2q}{4-q} < Q_d$, we have, again by Theorem 2.2,

$$\|H\nabla u\|^q_{L^q(\Omega)^d} \le \|\!|H|\!\|^q_{\frac{q\bar{q}}{\varepsilon}} \|\nabla u\|^q_{L^{\bar{q}}(\Omega)^d} \le C\|\!|H|\!\|^{\frac{p\varepsilon}{\bar{q}}}_p \|\nabla u\|^q_{L^{\bar{q}}(\Omega)^d} \le C\|\!|H|\!\|^q_p (\|f\|_{L^2(\Omega)} + \|g\|_{H^1(\Gamma)})^q.$$

The preceding estimates together give

$$\|R\|_{H^1(\Omega)} \le C\|\!|H|\!\|^2_p (\|f\|_{L^2(\Omega)} + \|g\|_{H^1(\Gamma)}),$$

completing the proof of the proposition. ∎

2.2. Well-posedness of problem (1.3). Note that the regularized functional J_γ involves only the $L^2(\Omega)^{d,d}$ penalty $\|\!|A|\!\|^2_2$, which is weaker than the commonly used Sobolev smooth penalty or total variation penalty, and does not induce very strong compactness to ensure the weak sequential closeness of the parameter-to-state map, which is commonly used for analyzing the well-posedness of the optimization problem [28]. To justify the approach, we employ the concept of H-convergence. First, we recall the concept of H-convergence [41] for elliptic problems with a zero Dirichlet boundary condition. Note that the H-limit is unique.

Definition 2.6. *A sequence $\{A^n\}_{n\in\mathbb{N}} \subset \mathcal{A}$ is said to be H-convergent to $A \in \mathcal{A}$, denoted by $A^n \xrightarrow{H} A$, if for all $f \in (H^1_0(\Omega))'$, we have $u_n \rightharpoonup u$ in $H^1(\Omega)$, and $A^n\nabla u_n \rightharpoonup A\nabla u$ in $L^2(\Omega)^d$, where u_n is the solution to*

$$\begin{cases} -\mathrm{div}(A^n\nabla u_n) = f & \text{in } \Omega, \\ u_n = 0 & \text{on } \Gamma, \end{cases}$$

and u solves the problem with A^n replaced by A.

The following version of the div-curl lemma plays an important role in the analysis.

Lemma 2.7. *Let $\{U_n = \nabla u_n\}_{n\in\mathbb{N}}$ and $\{V_n\}_{n\in\mathbb{N}}$ be two bounded sets in $L^2(\Omega)^d$ with $(u_n, V_n) \rightharpoonup (u_\infty, V_\infty)$ weakly in $H^1(\Omega) \times L^2(\Omega)^d$ and $\mathrm{div}V_n \to \mathrm{div}V_\infty$ strongly in $H^{-1}(\Omega)$. Then for any $\phi \in C^\infty_0(\Omega)$, we have*

$$\lim_{n\to\infty} \int_\Omega \phi\nabla u_n \cdot V_n dx = \int_\Omega \phi\nabla u_\infty \cdot V_\infty dx.$$

Proof. The proof can be found in [51, p. 91]. We sketch the proof for completeness. Since $\phi u_n \rightharpoonup \phi u_\infty$ in $H^1_0(\Omega)$, the strongly-weakly convergence in $\langle\cdot,\cdot\rangle_{H^{-1}(\Omega),H^1_0(\Omega)}$ implies

$$\lim_{n\to\infty} \langle \mathrm{div}V_n, \phi u_n\rangle_{H^{-1}(\Omega),H^1_0(\Omega)} = \langle \mathrm{div}V_\infty, \phi u_\infty\rangle_{H^{-1}(\Omega),H^1_0(\Omega)}.$$

This directly gives

$$\lim_{n\to\infty} (V_n, \phi\nabla u_n + u_n\nabla\phi)_{L^2(\Omega)^d} = (V_\infty, \phi\nabla u_\infty + u_\infty\nabla\phi)_{L^2(\Omega)^d}.$$

Meanwhile, by compact Sobolev embedding $H^1(\Omega) \hookrightarrow L^2(\Omega)$, $(V_n, u_n\nabla\phi)_{L^2(\Omega)^d}$ converges to $(V_\infty, u_\infty\nabla\phi)_{L^2(\Omega)^d}$, and the proof is completed. ∎

To prove the existence of a minimizer of problem (1.3), we need the following compactness result, which is the counterpart of H-convergence for a nonzero Dirichlet boundary condition.

Theorem 2.8. *For any sequence $\{A^n\}_{n\in\mathbb{N}} \subset \mathcal{A}$, there exists a subsequence, still denoted by $\{A^n\}$, and an element $A \in \mathcal{A}$ such that for every $(f, g) \in (H^1(\Omega))' \times H^{\frac{1}{2}}(\Gamma)$, there holds*

$$u_n \rightharpoonup u \text{ in } H^1(\Omega) \text{ and } A^n\nabla u_n \rightharpoonup A\nabla u \text{ in } L^2(\Omega)^d, \tag{2.6}$$

where u_n and u be are solutions of problem (1.1) with conductive matrices A^n and A, respectively.

Proof. Since $\{A^n\}_{n\in\mathbb{N}} \subset \mathcal{A}$, there exists a subsequence, still denoted by A^n, and $A \in \mathcal{A}$ such that $A^n \xrightarrow{H} A$ [51, Theorem 6.5]. First, we show that for any fixed $g \in H^{\frac{1}{2}}(\Gamma)$, there exists a subsequence of $\{A^n\}_{n\in\mathbb{N}}$, still denoted by $\{A^n\}_{n\in\mathbb{N}}$, such that (2.6) holds, following the argument of [51, Lemma 10.4]. We define the bilinear forms $a_n(\cdot,\cdot), a(\cdot,\cdot) : H^1(\Omega) \times H^1(\Omega) \to \mathbb{R}$ by

$$a_n(u, v) = (A^n\nabla u, \nabla v)_{L^2(\Omega)^d} \quad \text{and} \quad a(u, v) = (A\nabla u, \nabla v)_{L^2(\Omega)^d} \quad \forall u, v \in H^1(\Omega).$$

The weak formulation of problem (1.1) (with A^n) is to find $u_n \in K := \{u \in H^1(\Omega) : u = g \text{ on } \Gamma\}$ such that

$$a_n(u_n, v) = \langle f, v\rangle_{(H^1(\Omega))',H^1(\Omega)} \quad \forall v \in H^1_0(\Omega).$$

By Lemma 2.1, the sequence $\{u_n\}_{n\in\mathbb{N}}$ is uniformly bounded in $H^1(\Omega)$. Thus, we can extract a subsequence, again denoted by u_n, such that $u_n \rightharpoonup u$ in $H^1(\Omega)$. Since the set K is closed and convex, it is weakly closed, and we deduce $u \in K$. Since the space $C_c^\infty(\Omega)$ is dense in $L^2(\Omega)$, for any $\phi \in L^2(\Omega)^d$, there exists a sequence $\{\phi_\varepsilon\}_{\varepsilon>0} \subset C_c^\infty(\Omega)^d$ such that $\phi_\varepsilon \to \phi$ in $L^2(\Omega)^d$ as $\varepsilon \to 0^+$. For all $\phi \in L^2(\Omega)^d$,

$$\begin{aligned}|(\phi, A^n\nabla u_n - A\nabla u)_{L^2(\Omega)^d}| \le \|\phi - \phi_\varepsilon\|_{L^2(\Omega)^d}(\|A^n\nabla u_n\|_{L^2(\Omega)^d} + \|A\nabla u\|_{L^2(\Omega)^d})\\ + |(\phi_\varepsilon, A^n\nabla u_n - A\nabla u)_{L^2(\Omega)^d}|.\end{aligned}$$

By [51, Lemma 10.3], we obtain

$$A^n\nabla u_n \rightharpoonup A\nabla u \quad \text{in } L^2(\Omega)^d. \tag{2.7}$$

Next we show

$$a_n(u_n, u_n - v) \to a(u, u - v) \quad \forall v \in H^1(\Omega). \tag{2.8}$$

Since $A^n\nabla u_n \rightharpoonup A\nabla u, \nabla u_n \rightharpoonup \nabla u$ in $L^2(\Omega)^d$ and div $(A^n\nabla u_n) = f$, and curl $(\nabla u_n) = 0$, the div-curl lemma (cf. Lemma 2.7) implies

$$(\phi A^n\nabla u_n, \nabla u_n)_{L^2(\Omega)^d} \to (\phi A\nabla u, \nabla u)_{L^2(\Omega)^d} \quad \forall \phi \in C_c(\Omega). \tag{2.9}$$

Repeating the argument of [51, Lemma 10.4] and noting

$$a_n(u_n, v) \to a(u, v),$$

we obtain the assertion desired (2.8). Thus we have

$$a(u,v) = \langle f, v\rangle_{(H^1(\Omega))',H^1(\Omega)} \quad \forall v \in H_0^1(\Omega).$$

Next we apply a density/diagonal argument to show that for all $(f,g) \in (H^1(\Omega))' \times H^{\frac{1}{2}}(\Gamma)$, the assertion (2.6) holds. Since the space $H^{\frac{1}{2}}(\Gamma)$ is separable, there exists a countable dense subset G of $H^{\frac{1}{2}}(\Gamma)$. Let $\{0_n\} = \{n\}$. For any fixed $\{g^k\} \subset G$ $(k \geq 1)$, the preceding argument ensures the existence of a subsequence $\{(k)_n\} \subset \{(k-1)_n\}$ such that

$$u_{k_n}^k \rightharpoonup u^k \ \text{ in } \ H^1(\Omega) \quad \text{and} \quad A^{k_n}\nabla u_{k_n}^k \rightharpoonup A\nabla u^k \ \text{ in } \ L^2(\Omega)^d,$$

where $u_{k_n}^k$ and u^k satisfy

$$\begin{cases} -\operatorname{div}(A^{k_n}\nabla u_{k_n}^k) = f & \text{in } \Omega, \\ u_{k_n}^k = g^k & \text{on } \Gamma, \end{cases} \quad \text{and} \quad \begin{cases} -\operatorname{div}(A\nabla u^k) = f & \text{in } \Omega, \\ u^k = g^k & \text{on } \Gamma, \end{cases}$$

respectively. To show the convergence for any $(f,g) \in (H^1(\Omega))' \times H^{\frac{1}{2}}(\Gamma)$, we apply a diagonal argument, i.e., choosing the subsequence $\{k_k\}$, still denoted by A^n, i.e., $A^n \equiv A^{n_n}$. Since G is dense in $H^{\frac{1}{2}}(\Gamma)$, for any $g \in H^{\frac{1}{2}}(\Gamma)$ there exists $\{g^k\} \subset G$ such that $g^k \to g$ in $H^{\frac{1}{2}}(\Gamma)$. For any $\xi \in (H^1(\Omega))'$, we have

$$\begin{aligned} &\left|\langle \xi, u_n\rangle_{(H^1(\Omega))',H^1(\Omega)} - \langle \xi, u\rangle_{(H^1(\Omega))',H^1(\Omega)}\right| \\ &= \left|\langle \xi, u_n - u_n^k\rangle_{(H^1(\Omega))',H^1(\Omega)} + \langle \xi, u_n^k - u^k\rangle_{(H^1(\Omega))',H^1(\Omega)} + \langle \xi, u^k - u\rangle_{(H^1(\Omega))',H^1(\Omega)}\right| \\ &\leq \|\xi\|_{(H^1(\Omega))'}(\|u_n - u_n^k\|_{H^1(\Omega)} + \|u^k - u\|_{H^1(\Omega)}) + |\langle \xi, u_n^k - u^k\rangle_{(H^1(\Omega))',H^1(\Omega)}| \\ &\leq C\|g - g^k\|_{H^{\frac{1}{2}}(\Gamma)} + |\langle \xi, u_n^k - u^k\rangle_{(H^1(\Omega))',H^1(\Omega)}|, \end{aligned}$$

which yields $u_n \rightharpoonup u$ in $H^1(\Omega)$. Since $\|A^n\nabla u_n - A^n\nabla u_n^k\|_{L^2(\Omega)^d} \leq C\|u_n - u_n^k\|_{H^1(\Omega)}$ and repeating the argument gives $A^n\nabla u_n \rightharpoonup A\nabla u$ in $L^2(\Omega)^d$. This completes the proof of the theorem. ∎

Theorem 2.8 gives the the H-convergence for a nonzero Dirichlet boundary data, and further, the H-limit for the nonzero Dirichlet boundary condition case is identical with the zero case. The next lemma gives the norm inequality for the H-limit [41].

Lemma 2.9. *Let the sequence $\{A^n\}_{n\in\mathbb{N}} \subset \mathcal{A}$ be $A^n \xrightarrow{H} A$ and $A^n \overset{*}{\rightharpoonup} A^0$ in $L^\infty(\Omega)^{d,d}$. Then*

$$A \leq A^0 \ \text{a.e. in } \Omega \quad \text{and} \quad |||A|||_2^2 \leq |||A^0|||_2^2 \leq \liminf_{n\to\infty} |||A^n|||_2^2. \tag{2.10}$$

With the compactness result in Theorem 2.8, we can state the existence of a minimizer.

Theorem 2.10. *There exists at least one minimizer to problem* (1.3).

Proof. The functional J_γ is bounded from below by zero, and thus we can find a minimizing sequence $\{A^n\}_{n\in\mathbb{N}} \subset \mathcal{A}$ such that

$$\lim_{n\to\infty} J_\gamma(A^n) = \inf_{A\in\mathcal{A}} J_\gamma(A).$$

By Theorem 2.8, since the sequence $\{A^n\}_{n\in\mathbb{N}}$ is bounded in $L^\infty(\Omega)^{d,d}$, there exists a subsequence $\{A^{n_k}\}_{k\in\mathbb{N}}$ and some $A \in \mathcal{A}$ such that $A^{n_k} \xrightarrow{H} A$ in $L^\infty(\Omega)^{d,d}$. Letting $u^\ell_{n_k} = u^\ell(A^{n_k}), \ell = 1,\dots,L$, we have $u^\ell_{n_k} \rightharpoonup u^\ell(A), \ell = 1,\dots,L$ in $H^1(\Omega)$. Hence, the weak lower semicontinuity of the $L^2(\Omega)$-norm and Lemma 2.9 give

$$\begin{aligned} J_\gamma(A) &= \frac{1}{2}\sum_{\ell=1}^{L} \|A\nabla u^\ell - \vec{h}^\ell\|^2_{L^2(\Omega)^d} + \frac{\gamma}{2}|||A|||_2^2 \\ &\le \frac{1}{2}\liminf_{n'\to\infty} \sum_{\ell=1}^{L} \|A^{n'}\nabla u^\ell_{n'} - \vec{h}^\ell\|^2_{L^2(\Omega)^d} + \frac{\gamma}{2}\liminf_{n'\to\infty} |||A^{n'}|||_2^2 \\ &\le \liminf_{n'\to\infty} J_\gamma(A^{n'}) = \inf_{A\in\mathcal{A}} J_\gamma(A). \end{aligned}$$

Thus, A is a global minimizer. This completes the proof of the theorem. ∎

Next we derive the expression of the gradient J'_γ of the functional J_γ and the first-order necessary optimality system using the adjoint technique. The former allows applying popular gradient-descent type algorithms, whereas the latter is useful for designing Newton type methods. Let the adjoint variable $\bar{p}^\ell$, $\ell = 1,\dots,L$, solve

$$\begin{cases} -\mathrm{div}(A\nabla\bar{p}^\ell) = \mathrm{div}(A(A\nabla u^\ell - \vec{h}^\ell)) & \text{in } \Omega, \\ \bar{p}^\ell = 0 & \text{on } \Gamma. \end{cases} \tag{2.11}$$

We show the differentiability of $J_\gamma(A)$ in the $L^p(\Omega)^{d,d}$ topology. For two vectors $a, b \in \mathbb{R}^d$, we denote the symmetrized tensor product by $(a\otimes b)_{ij} = \frac{1}{2}(a_ib_j + a_jb_i)$, $i,j = 1,\dots,d$, and the Frobenius inner product between two matrices $A, B \in \mathbb{R}^d$ by $A\cdot B$. The lengthy but routine proof is deferred to the appendix.

Theorem 2.11. *Letting $\bar{p}^\ell$ be defined in (2.11), for any $H \in L^\infty(\Omega)^{d,d}$ such that $A+tH \in \mathcal{A}$ for sufficiently small $t > 0$, the directional derivative $J'_\gamma(A)[H]$ of J_γ is given by*

$$J'_\gamma(A)[H] = \int_\Omega \left(\sum_{\ell=1}^{L}\left(\nabla u^\ell\otimes\nabla\bar{p}^\ell + \nabla u^\ell\otimes\left(A\nabla u^\ell - \vec{h}^\ell\right) + \gamma A\right)\right)\cdot H dx. \tag{2.12}$$

Moreover, if A is an interior point of $\mathcal{A}$, then $J_\gamma(A)$ is Fréchet differentiable in the $L^p(\Omega)^{d,d}$ topology for any $p \in (\frac{4Q_d}{Q_d-2}, \infty]$.

Next we derive the first-order necessary optimality system of problem (1.3). Recall the subset $K := \{A \in \mathcal{S}_d | \alpha I \le A \le \beta I\} \subset \mathcal{S}_d$ given in (1.2), with $A \le B$ indicating that $B - A$ is symmetric positive semidefinite. Since K is a convex and closed subset of $\mathcal{S}_d$, we can define an orthogonal projection $P_K : \mathcal{S}_d \to K$, characterized by the following variational inequality:

$$(A - P_K(A))\cdot(B - P_K(A)) \le 0 \quad \forall B \in K.$$

Theorem 2.12. *Let $A^* \in \mathcal{A}$ solve problem (1.3); then the tuple $(A^*, u^\ell, \bar{p}^\ell)$ satisfies the following optimality system, for every $\lambda > 0$,*

$$\text{primal} \quad \begin{cases} -\operatorname{div}(A^*\nabla u^\ell) = f^\ell & \text{in } \Omega, \\ u^\ell = g^\ell & \text{on } \Gamma, \end{cases}$$

$$\text{dual} \quad \begin{cases} -\operatorname{div}(A^*\nabla p^\ell) = \operatorname{div}(A^*(A^*\nabla u^\ell - \vec{h}^\ell)) & \text{in } \Omega, \\ p^\ell = 0 & \text{on } \Gamma, \end{cases}$$

complementarity

$$A^*(x) = P_K\Big(A^* - \lambda \sum_{\ell=1}^{L} (\nabla u^\ell \otimes (A^*\nabla u^\ell - \vec{h}^\ell) + \nabla u^\ell \otimes \nabla p^\ell + \gamma A^*)\Big) \text{ a.e. in } \Omega.$$

Proof. The optimality of A^* implies $J'_\gamma(A^*)(B - A^*) \geq 0$ for all $B \in \mathcal{A}$. In view of (2.12), it can be rewritten as

$$\int_\Omega \Big(A^* - \lambda \sum_{\ell=1}^{L} \big(\nabla u^\ell \otimes (A^*\nabla u^\ell - \vec{h}^\ell) + \nabla u^\ell \otimes \nabla p^\ell + \gamma A^*\big) - A^*\Big) \cdot (B - A^*) dx \leq 0 \quad \forall B \in \mathcal{A}.$$

The inequality is equivalent to

$$A^* = P_{\mathcal{A}}\Big(A^* - \lambda \sum_{\ell=1}^{L} \big(\nabla u^\ell \otimes (A^*\nabla u^\ell - \vec{h}^\ell) + \nabla u^\ell \otimes \nabla p^\ell + \gamma A^*\big)\Big), \tag{2.13}$$

since $P_{\mathcal{A}}$ is a projection onto a closed convex subset in a Hilbert space. Now for every $x \in \Omega$,

$$\begin{aligned} &P_K\Big(A^*(x) - \lambda \sum_{\ell=1}^{L} \big(\nabla u^\ell(x) \otimes (A^*(x)\nabla u^\ell(x) - \vec{h}^\ell(x)) + \nabla u^\ell(x) \otimes \nabla p^\ell(x) + \gamma A^*(x)\big)\Big) \\ &= \arg\min_{B \in K} \Big|\Big|\Big|A^*(x) - \lambda \sum_{\ell=1}^{L} \big(\nabla u^\ell(x) \otimes (A^*(x)\nabla u^\ell(x) - \vec{h}^\ell(x)) + \nabla u^\ell(x) \otimes \nabla p^\ell(x) \\ &\quad + \gamma A^*(x)\big) - B\Big|\Big|\Big|_p. \end{aligned}$$

This and the uniqueness of a projection onto convex sets imply that the relation (2.13) is indeed equivalent to the pointwise projection $A^*(x) = P_K(A^*(x) - \lambda \sum_{\ell=1}^{L} (\nabla u^\ell(x) \otimes (A^*(x)\nabla u^\ell(x) - \vec{h}^\ell(x)) + \nabla u^\ell(x) \otimes \nabla p^\ell(x) + \gamma A^*(x)))$ a.e. in Ω, which directly implies the desired complementary condition. ∎

Remark 2.13. Choosing $\lambda = \frac{1}{\gamma}$ in the complementarity condition gives

$$A^*(x) = P_K\Big(-\gamma^{-1} \sum_{\ell=1}^{L} \nabla u^\ell \otimes (A^*\nabla u^\ell - \vec{h}^\ell) + \nabla u^\ell \otimes \nabla p^\ell\Big) \quad \text{a.e. in } \Omega. \tag{2.14}$$

This choice is employed in the numerical implementation in section 5.

Last, we state a convergence result with respect to the noise level. Suppose that we are given a set of noisy measurements $\vec{h}^{\ell,\delta} \in L^2(\Omega)^d, \ell = 1, \ldots, L$, with a noise level δ, i.e.,

$$\|\vec{h}^{\ell} - \vec{h}^{\ell,\delta}\|_{L^2(\Omega)^d} \leq \delta, \quad \ell = 1, \ldots, L. \tag{2.15}$$

Accordingly, consider the following optimization problem:

$$\min_{A\in\mathcal{A}} \left\{ J_\gamma^\delta(A) := \frac{1}{2}\sum_{\ell=1}^{L} \|A\nabla u^\ell(A) - \vec{h}^{\ell,\delta}\|_{L^2(\Omega)^d}^2 + \frac{\gamma}{2}|||A|||_2^2 \right\}. \tag{2.16}$$

The next result shows the convergence of regularized solutions to a minimum norm solution as the noise level δ tends to zero, i.e., regularizing property of problem (1.3). The minimum norm solution $A^\dagger$ is defined by $A^\dagger \in \arg\min_{A\in\mathcal{I}_{\mathcal{A}}(\vec{h}^L)} |||A|||_2^2$, where $\mathcal{I}_{\mathcal{A}}(\vec{h}, L) = \{A \in \mathcal{A} | \vec{h}^\ell = A\nabla u^\ell(A), \ell = 1, \ldots, L\}$ is assumed to be nonempty. This result ensures that the solutions to the regularized problem (1.3) don't differ too much from the reference solution, provided that the noise level δ is sufficiently small and the regularization parameter γ is chosen properly.

Theorem 2.14. *Let $\vec{h}^{\ell,\delta}$ satisfy (2.15), let $A^\delta \in \mathcal{A}$ be a solution of problem (2.16), and suppose that $\gamma \to 0$ and $\frac{\delta}{\sqrt{\gamma}} \to 0$, as $\delta \to 0$. Then up to a subsequence, there holds $A^\delta \to A$ in $L^2(\Omega)^{d,d}$ as $\delta \to 0$ for some minimum norm solution A.*

Proof. Given a sequence $\{\delta_k\}_{k\in\mathbb{N}}$ with $\lim_{k\to\infty} \delta_k = 0$, we choose $\gamma_k > 0$ such that $\lim_{k\to\infty} \gamma_k = 0$ and $\lim_{k\to\infty} \gamma_k^{-\frac{1}{2}}\delta_k = 0$. Further, let $A_k := A_{\gamma_k}^{\delta_k} \in \mathcal{A}$ be a minimizer of $J_{\gamma_k}^{\delta_k}(A)$ over $\mathcal{A}$. For any minimum norm solution $A^\dagger \in \mathcal{A}$, there holds $J_{\gamma_k}^{\delta_k}(A_k) \leq J_{\gamma_k}^{\delta_k}(A^\dagger)$. That is,

$$\begin{aligned} &\frac{1}{2}\sum_{\ell=1}^{L} \|A_k\nabla u^\ell(A_k) - \vec{h}^{\ell,\delta_k}\|_{L^2(\Omega)^d}^2 + \frac{\gamma_k}{2}|||A_k|||_2^2 \\ &\leq \frac{1}{2}\sum_{\ell=1}^{L} \|A^\dagger\nabla u^\ell(A^\dagger) - \vec{h}^{\ell,\delta_k}\|_{L^2(\Omega)^d}^2 + \frac{\gamma_k}{2}\|A^\dagger\|_{L^2(\Omega)^{d,d}}^2 \\ &\leq \frac{L}{2}\delta_k^2 + \frac{\gamma_k}{2}|||A^\dagger|||_2^2. \end{aligned} \tag{2.17}$$

This and the condition on γ_k imply

$$\limsup_{k\to\infty} |||A_k|||_2^2 \leq \limsup_{k\to\infty} (L\gamma_k^{-1}\delta_k^2 + |||A^\dagger|||_2^2) = |||A^\dagger|||_2^2. \tag{2.18}$$

By Theorem 2.8, there exists a subsequence, again denoted by $\{A_k\}_{k\in\mathbb{N}}$, $A, A^0 \in \mathcal{A}$, such that $A_k \xrightarrow{H} A$ and $A_k \to A^0$ weak $*$ in $L^\infty(\Omega)^{d,d}$. Lemma 2.9 implies

$$A \leq A^0 \text{ a.e. in } \Omega \quad \text{and} \quad |||A|||_2^2 \leq |||A_0|||_2^2 \leq \liminf_{k\to\infty} |||A_k|||_2^2. \tag{2.19}$$

By the definition of H-convergence, we have $u^\ell(A_k) \rightharpoonup u^\ell(A)$ in $H^1(\Omega)$, $A_k\nabla u^\ell(A_k) \rightharpoonup A\nabla u^\ell(A)$ in $L^2(\Omega)^d$. Since $\|\vec{h}^\ell - \vec{h}^{\ell,\delta_k}\|_{L^2(\Omega)^d} \leq \delta_k$, from the estimate (2.17), we deduce

$$\sum_{\ell=1}^{L} \|A\nabla u^\ell(A) - \vec{h}^\ell\|_{L^2(\Omega)^d} \leq \liminf_{k\to\infty} \sum_{\ell=1}^{L} \|A_k\nabla u^\ell(A_k) - \vec{h}^{\ell,\delta_k}\|_{L^2(\Omega)^d} = 0. \tag{2.20}$$

Therefore, $A \in \mathcal{I}_{\mathcal{A}}(\vec{h}, L)$, and it is a minimum norm solution. From (2.18) it follows that $A_k \to A^0$ weak $*$ in $L^\infty(\Omega)^{d,d}$ and $A \le A^0$ a.e. in Ω. Then we have

$$\begin{aligned}\limsup_{k\to\infty} |||A_k - A|||_2^2 &= \limsup_{k\to\infty}(|||A_k|||_2^2 + |||A|||_2^2) - 2(A_k, A)_{L^2(\Omega)^{d,d}} \\ &\le 2|||A|||_2^2 - 2(A_0, A)_{L^2(\Omega)^{d,d}} \le 0.\end{aligned}$$

In conclusion, $A_k \to A$ in $L^2(\Omega)^{d,d}$ as $k \to \infty$, and A is a minimum norm solution. ∎

Remark 2.15. Note that the minimum norm solution $A^\dagger$ is generally nonunique, and it does not necessarily coincide with the exact conductivity tensor. Nonetheless, it coincides with the exact conductivity tensor if the set $\mathcal{I}_{\mathcal{A}}(\vec{h}, L)$ consists of one singleton. Under suitable regularity conditions on the problem data and given a sufficient number of current densities, the anisotropic conductivity tensor is uniquely determined [8, 7]. Then the set $\mathcal{I}_{\mathcal{A}}(\vec{h}, L)$ consists of one single element, and accordingly, the minimum norm solution is unique, and also by the standard subsequence argument, the whole sequence converges to the unique minimum norm solution as $\delta \to 0^+$.

3. Numerical discretization and convergence.

In practice, numerically solving problem (1.3) requires suitable discretization. Since the problem involves variable coefficients, it is most conveniently carried out using the Galerkin finite element method [13, 12]. Throughout, we assume that the domain Ω is a polygon in two dimensions or polyhedron in three dimensions. Let $\mathcal{T}$ be a quasi-uniform triangulation of the domain Ω with a maximum mesh size h. We employ the piecewise linear finite element spaces $V_h \subset H^1(\Omega)$ and $X_h \subset L^2(\Omega)$ defined respectively by

$$\begin{aligned}V_h &= \{v_h \in C(\overline{\Omega}) : v_h|_T \in P_1(T) \quad \forall T \in \mathcal{T}\},\\ X_h &= \{A_h : (A_h)_{i,j} \in L^2(\Omega), (A_h)_{i,j}|_T \in P_1(T), i, j = 1, \ldots, d, \forall T \in \mathcal{T}\},\end{aligned}$$

where $P_1(T)$ consists of all linear functions over T. The discrete admissible set $\mathcal{A}_h$ is given by $\mathcal{A}_h = \mathcal{A} \cap X_h$. Let $V_{h,0} = V_h \cap H_0^1(\Omega) \subset V_h$, whose elements vanish on the boundary Γ, and denote by $V_h(\Gamma)$ the trace space of V_h on Γ. Let $P_h : L^2(\Omega) \to V_{h,0}$ be the standard $L^2(\Omega)$ orthogonal projection. Then it is $H^1(\Omega)$-stable [11], i.e.,

$$\|P_h(u - \tilde{u})\|_{H_0^1(\Omega)} \le C\|u - \tilde{u}\|_{H_0^1(\Omega)}.$$

To formulate the finite element approximation of problem (1.1), we fix a function $g_h \in V_h(\Gamma)$ which approximates the given Dirichlet boundary condition g. Then the finite element problem for problem (1.1) reads, Find $u_h \in V_h$ such that $u_h = g_h$ on Γ and

$$(A_h \nabla u_h, \nabla v_h)_{L^2(\Omega)^d} = (f, v_h)_{L^2(\Omega)} \quad \forall v_h \in V_{h,0}. \tag{3.1}$$

This defines a discrete forward operator $F_h : A_h \to u_h$ (again suppressing the dependence on the problem data (f, g)).

Remark 3.1. Since the space $V_h(\Gamma)$ is dense in $H^{\frac{1}{2}}(\Gamma)$, there exists $g_h \in V_h(\Gamma)$ such that $\|g_h - g\|_{H^{\frac{1}{2}}(\Gamma)} \to 0$ as $h \to 0$. If $g \in H^{\frac{3}{2}}(\Gamma)$, a standard choice for the Dirichlet data $g_h \in V_h(\Gamma)$ is the Lagrange interpolation $I_h g$ of g [13, 12]. If $g \in H^{\frac{1}{2}}(\Gamma)$, we may let g_h be the $L^2(\Gamma)$-projection of g onto $V_h(\Gamma)$ [20, 9].

Throughout, we take $g_h = \tilde{u}_h|_\Gamma$, with $\tilde{u}_h \in V_h$ and $\|\tilde{u}_h - \tilde{u}\|_{H^1(\Omega)} \to 0$, where $\tilde{u}$ satisfies $-\Delta\tilde{u} = 0$ in Ω and $\tilde{u}|_\Gamma = g$ (i.e., $\tilde{u}$ is the harmonic extension of g from the boundary Γ to the domain Ω). Then by [13, p. 143] and [50, p. 200] and the density of V_h in $H^1(\Omega)$, $V_{h,0}$ in $H_0^1(\Omega)$, we have

$$\begin{aligned}\|u - u_h\|_{H^1(\Omega)} &\le \beta^{\frac{1}{2}}\alpha^{-\frac{1}{2}} \inf_{v_h \in V_{h,0}} \|u - (\tilde{u}_h + v_h)\|_{H^1(\Omega)}\\ &\le \beta^{\frac{1}{2}}\alpha^{-\frac{1}{2}}\big(\inf_{v_h \in V_{h,0}} \|u - \tilde{u} - v_h\|_{H_0^1(\Omega)} + \|\tilde{u} - \tilde{u}_h\|_{H^1(\Omega)}\big).\end{aligned}$$

Upon choosing $v_h = P_h(u - \tilde{u}) \in V_{h,0}$, then we have

$$\begin{aligned}\|u_h\|_{H^1(\Omega)} &\le \|u - u_h\|_{H^1(\Omega)} + \|u\|_{H^1(\Omega)}\\ &\le \beta^{\frac{1}{2}}\alpha^{-\frac{1}{2}}(2\|u - \tilde{u}\|_{H_0^1(\Omega)} + \|\tilde{u} - \tilde{u}_h\|_{H^1(\Omega)}) + \|u\|_{H^1(\Omega)}.\end{aligned}$$

Thus, $\|u_h\|_{H^1(\Omega)}$ is uniformly bounded. This fact will be frequently used below.

Now we can formulate the discrete counterpart of problem (1.3):

$$\min_{A_h \in \mathcal{A}_h} \left\{ J_{\gamma,h}(A_h) := \frac{1}{2}\sum_{\ell=1}^{L} \|A_h \nabla u_h^\ell(A_h) - \vec{h}^\ell\|_{L^2(\Omega)^d}^2 + \frac{\gamma}{2}|||A_h|||_2^2 \right\}. \tag{3.2}$$

3.1. Convergence analysis. To analyze the convergence of problem (3.2), we use the concept of Hd-convergence defined below. It was introduced in [19] and [14] in the context of finite volume and finite element discretizations of boundary value problems, respectively, to adapt H-convergence results to a discrete setting.

Definition 3.2 ([14]). *A sequence $\{A_h\} \subset \mathcal{A}$ is said to be Hd-convergent to $A \in \mathcal{A}$, denoted by $A_h \xrightarrow{Hd} A$, if for all $f \in H^{-1}(\Omega)$, we have $u_h \rightharpoonup u$ in $H^1(\Omega)$, and $A_h\nabla u_h \rightharpoonup A\nabla u$ in $L^2(\Omega)^d$, where $u_h \in V_{h,0}$ is the finite element solution to*

$$(A_h\nabla u_h, \nabla v_h)_{L^2(\Omega)^d} = \langle f, v_h\rangle_{H^{-1}(\Omega),H_0^1(\Omega)} \quad \forall v_h \in V_{h,0},$$

and u solves $-\mathrm{div}(A\nabla u) = f$ in Ω and $u = 0$ on the boundary Γ.

Next we establish the Hd-convergence for a nonzero Dirichlet boundary condition, which will be useful for the convergence analysis of the discrete problem (3.2).

Theorem 3.3. *Assume that $\{A_h \in \mathcal{A}_h\}_{h>0} \subset \mathcal{A}$ with $A_h \xrightarrow{Hd} A$ for any given $f \in H^{-1}(\Omega)$, $g \in H^{\frac{1}{2}}(\Gamma)$, $g_h \in V_h(\Gamma)$ with $\|g_h - g\|_{H^{\frac{1}{2}}(\Gamma)} \to 0$. Let $u_h \in V_h$ and $u \in H^1(\Omega)$ be the solutions of the following finite element problem and the elliptic problem (1.1), respectively: $u_h \in V_h$ with $u_h|_\Gamma = g_h$ with*

$$(A_h\nabla u_h, \nabla v_h)_{L^2(\Omega)^d} = \langle f, v_h\rangle_{H^{-1}(\Omega),H_0^1(\Omega)} \quad \forall v_h \in V_{h,0},$$

and u solves $-\mathrm{div}(A\nabla u) = f$ in Ω and $u = g$ on the boundary Γ. Then there holds

$$u_h \rightharpoonup u \text{ in } H^1(\Omega) \text{ and } A_h\nabla u_h \rightharpoonup A\nabla u \text{ in } L^2(\Omega)^d.$$

Proof. Let $\bar{u} \in H^1(\Omega)$ with $\bar{u}|_\Gamma = g$. Then

$$(A\nabla(u-\bar{u}), \nabla v)_{L^2(\Omega)^d} = \langle f + \mathrm{div} A\nabla\bar{u}, v\rangle_{H^{-1}(\Omega), H_0^1(\Omega)} \quad \forall v \in H_0^1(\Omega).$$

Let $z_h \in V_{h,0}$ be the solution to the finite element problem

$$(A_h\nabla z_h, \nabla v_h)_{L^2\Omega^d} = \langle f + \mathrm{div} A\nabla\bar{u}, v_h\rangle_{H^{-1}(\Omega), H_0^1(\Omega)} \quad \forall v_h \in V_{h,0}.$$

By the Hd-convergence [14, Theorem 3.1], we have (up to a subsequence)

$$z_h \rightharpoonup u - \bar{u} \text{ in } H_0^1(\Omega) \quad \text{and} \quad A_h\nabla z_h \rightharpoonup A\nabla(u-\bar{u}) \text{ in } L^2(\Omega)^d. \tag{3.3}$$

We denote by $\bar{u}_h \in V_h$ with $\bar{u}_h|_\Gamma = g_h$ and

$$(A_h\nabla\bar{u}_h, \nabla v_h)_{L^2\Omega^d} = \langle -\mathrm{div} A\nabla\bar{u}, v_h\rangle_{H^{-1}(\Omega), H_0^1(\Omega)} = (A\nabla\bar{u}, \nabla v_h)_{L^2\Omega^d} \quad \forall v_h \in V_{h,0}.$$

By definition, $A_h\nabla\bar{u}_h$ is the $L^2(\Omega)$-projection of $A\nabla\bar{u}$ onto the space $\nabla V_{h,0} := \{\nabla v_h : v_h \in V_{h,0}\}$. Since $\nabla V_{h,0}$ is the standard piecewise constant finite element space and it is dense in $L^2(\Omega)^d$ space, we deduce

$$A_h\nabla\bar{u}_h \rightharpoonup A\nabla\bar{u} \quad \text{in } L^2(\Omega)^d. \tag{3.4}$$

Meanwhile, by the definition of u_h, we can split u_h into $u_h = z_h + \bar{u}_h$, and furthermore, in view of (3.3)–(3.4), we have $A_h\nabla u_h \rightharpoonup A\nabla u$ in $L^2(\Omega)^d$. It remains to show that $u_n \rightharpoonup u$ in $H^1(\Omega)$. Since the sequence $\{u_h\}_{h>0}$ is bounded in $H^1(\Omega)$, there exists a weak accumulation point $\hat{u} \in H^1(\Omega)$, and it suffices to prove $\hat{u} = u$. Then up to a subsequence, let $u_h \rightharpoonup \hat{u}$ in $H_0^1(\Omega)$. For any $\hat{f} \in H^{-1}(\Omega)$, let $y_h \in V_{h,0}$ and $y \in H_0^1(\Omega)$ be solutions to the finite element discretization and the continuous PDE, respectively, i.e.,

$$\begin{aligned}(A_h\nabla y_h, \nabla v_h)_{L^2(\Omega)^d} &= \langle \hat{f}, v_h\rangle_{H^{-1}(\Omega), H_0^1(\Omega)} \quad \forall v_h \in V_{h,0},\\ (A\nabla y, \nabla v)_{L^2(\Omega)^d} &= \langle \hat{f}, v\rangle_{H^{-1}(\Omega), H_0^1(\Omega)} \quad \forall v \in H_0^1(\Omega).\end{aligned}$$

Then the Hd-convergence [14, Theorem 3.1] implies $y_h \rightharpoonup y$ in $H_0^1(\Omega)$, $A_h\nabla y_h \rightharpoonup A\nabla y$ in $L^2(\Omega)^d$. For any given $\phi \in C_0^\infty(\Omega)$, we define

$$E_h = (\phi A_h\nabla y_h, \nabla u_h)_{L^2(\Omega)^d}.$$

Then direct computation gives

$$\begin{aligned}E_h &= (A_h\nabla y_h, \phi\nabla u_h)_{L^2(\Omega)^d}\\ &= (A_h\nabla y_h, \nabla(\phi u_h))_{L^2(\Omega)^d} - (A_h\nabla y_h, u_h\nabla\phi)_{L^2(\Omega)^d}\\ &= (A_h\nabla y_h, \nabla I_h(\phi u_h))_{L^2(\Omega)^d} - (A_h\nabla y_h, u_h\nabla\phi)_{L^2(\Omega)^d}\\ &\quad +(A_h\nabla y_h, \nabla(\phi u_h - I_h(\phi u_h)))_{L^2(\Omega)^d}.\end{aligned}$$

Then using the weak formulation of y_h, we obtain

$$E_h = \langle \hat{f}, I_h(\phi u_h)\rangle_{H^{-1}(\Omega),H_0^1(\Omega)} - (A_h\nabla y_h, u_h\nabla\phi)_{L^2(\Omega)^d} + (A_h\nabla y_h, \nabla(\phi u_h - I_h(\phi u_h)))_{L^2(\Omega)^d}, \tag{3.5}$$

where I_h denotes the standard Lagrange interpolation operator. Then there hold

$$I_h(\phi u_h) \rightharpoonup \phi\hat{u} \text{ in } H_0^1(\Omega) \quad \text{and} \quad \|\phi u_h - I_h(\phi u_h)\|_{H^1(\Omega)} \to 0.$$

Indeed, by the standard interpolation estimate [12], we have

$$\|\phi u_h - I_h(\phi u_h)\|_{H^1(T)} \le Ch\|D^2(\phi u_h)\|_{L^2(T)} \le ch\|\phi\|_{W^{2,\infty}(T)}\|u_h\|_{H^1(T)} \quad \forall T \in \mathcal{T},$$

so that $\phi u_h - I_h(\phi u_h) \to 0$ in $H_0^1(\Omega)$ as $h \to 0^+$ since $\|u_h\|_{H^1(\Omega)} \le C$. This and the weak convergence $\phi u_h \rightharpoonup \phi\hat{u}$ imply $I_h(\phi u_h) \rightharpoonup \phi\hat{u}$. Upon passing to the limit $h \to 0^+$ in the identity (3.5), we obtain

$$\begin{aligned}\lim_{h\to 0^+} E_h &= \langle \hat{f}, \phi\hat{u}\rangle_{H^{-1}(\Omega),H_0^1(\Omega)} - (A\nabla y, \hat{u}\nabla\phi)_{L^2(\Omega)^d}\\ &= \langle -\mathrm{div}(A\nabla y), \phi\hat{u}\rangle_{H^{-1}(\Omega),H_0^1(\Omega)} - (A\nabla y, \hat{u}\nabla\phi)_{L^2(\Omega)^d}\\ &= (A\nabla y, \phi\nabla\hat{u})_{L^2(\Omega)^d}.\end{aligned}$$

Likewise, repeating the preceding argument yields

$$\begin{aligned}E_h &= (A_h\nabla u_h, \phi\nabla y_h)_{L^2(\Omega)^d}\\ &= (A_h\nabla u_h, \nabla(\phi y_h))_{L^2(\Omega)^d} - (A_h\nabla u_h, y_h\nabla\phi)_{L^2(\Omega)^d}\\ &= (A_h\nabla u_h, \nabla I_h(\phi y_h))_{L^2(\Omega)^d} - (A_h\nabla u_h, y_h\nabla\phi)_{L^2(\Omega)^d}\\ &\quad +(A_h\nabla u_h, \nabla(\phi y_h - I_h(\phi y_h)))_{L^2(\Omega)^d}\\ &= \langle f, I_h(\phi y_h)\rangle_{H^{-1}(\Omega),H_0^1(\Omega)} - (A_h\nabla u_h, y_h\nabla\phi)_{L^2(\Omega)^d}\\ &\quad +(A_h\nabla u_h, \nabla(\phi y_h - I_h(\phi y_h)))_{L^2(\Omega)^d}.\end{aligned}$$

Passing to the limit $h \to 0^+$ in the last identity gives

$$\begin{aligned}\lim_{h\to 0^+} E_h &= \langle f, \phi y\rangle_{H^{-1}(\Omega),H_0^1(\Omega)} - (A\nabla u, y\nabla\phi)_{L^2(\Omega)^d}\\ &= \langle -\mathrm{div}(A\nabla u), \phi y\rangle_{H^{-1}(\Omega),H_0^1(\Omega)} - (A\nabla u, y\nabla\phi)_{L^2(\Omega)^d}\\ &= (A\nabla u, \phi\nabla y)_{L^2(\Omega)^d}.\end{aligned}$$

Since the two limits are identical, we conclude

$$(A\nabla y, \phi\nabla\hat{u})_{L^2(\Omega)^d} = (A\nabla u, \phi\nabla y)_{L^2(\Omega)^d}.$$

Since the choice of the functions $\hat{f}$ and ϕ is arbitrary, we have $\nabla u = \nabla\hat{u}$. Since $u_h \rightharpoonup \hat{u}$ weakly in $H^1(\Omega)$, by the Sobolev embedding theorem and trace theorem, u_h converges to u strongly in $L^2(\Gamma)$, i.e., $\|\hat{u}|_\Gamma - g_h\|_{L^2(\Gamma)} \to 0$. This directly gives $\hat{u}|_\Gamma = g = u|_\Gamma$. Together with the identity $\nabla u = \nabla\hat{u}$, we obtain $u = \hat{u}$, which completes the proof of the theorem. ∎

The next result is a discrete analogue of Lemma 2.9 [14, Corollary 3.1].

Lemma 3.4. *Let the sequence* $\{A_h\}_{h>0}$ *be* $A_h \xrightarrow{Hd} A$ *and* $A_h \overset{*}{\rightharpoonup} A^0$ *in* $L^\infty(\Omega)^{d,d}$. *Then*

$$A \le A^0 \quad \text{a.e. in } \Omega \quad \text{and} \quad |||A|||_2^2 \le |||A^0|||_2^2 \le \liminf_{h\to 0} |||A_h|||_2^2.$$

Now we can state a convergence result for a sequence $\{A_h\}_{h>0}$ of solutions of the discrete problem (3.2). It is a finite element version of the result obtained in [19].

Theorem 3.5. *There exists at least one solution* $A_h \in \mathcal{A}_h$ *to problem* (3.2). *Further, there exists a subsequence* $\{A_{h'}\}_{h'>0}$ *and* $A \in \mathcal{A}$ *such that* $A_{h'} \to A$ *in* $L^2(\Omega)^{d,d}$ *and* A *is a solution of problem* (1.3).

Proof. Problem (3.2) is a finite-dimensional optimization problem, and the existence of a minimizer A_h follows directly from the coercivity and continuity of the functional $J_{\gamma,h}$. It remains to prove the convergence. By Theorem 3.3 and Lemma 3.4, there exists a subsequence $\{A_{h'} \in \mathcal{A}_{h'}\}_{h'>0}$ and $A \in \mathcal{A}$ such that $A_{h'} \xrightarrow{Hd} A$ and $A_{h'} \overset{*}{\rightharpoonup} A^0$ in $L^\infty(\Omega)^{d,d}$, and

$$A \le A^0 \text{ a.e. in } \Omega, \quad \text{and} \quad |||A|||_2^2 \le \liminf_{k\to\infty} |||A_{h'}|||_2^2. \tag{3.6}$$

Let $u_{h'}^\ell(A_{h'}) = F_{h'}^\ell(A_{h'})$, $u^\ell(A) = F^\ell(A)$, $i = 1, \dots, M$. Then we have

$$u_{h'}^\ell(A_{h'}) \rightharpoonup u^\ell(A) \text{ in } H^1(\Omega), \quad \text{and} \quad A_{h'}\nabla u_{h'}^\ell \rightharpoonup A\nabla u^\ell \text{ in } L^2(\Omega)^d.$$

The argument of Theorem 2.10 implies

$$J_\gamma(A) \le \liminf_{h'\to 0} J_{\gamma,h'}(A_{h'}).$$

Next, Theorem 2.10 implies that problem (1.3) has a solution $\tilde{A} \in \mathcal{A}$. Then we have

$$J_\gamma(\tilde{A}) \le J_\gamma(A) \le \liminf_{h'\to 0} J_{\gamma,h'}(A_{h'}) \le \limsup_{h'\to 0} J_{\gamma,h'}(A_{h'}) \le \limsup_{h'\to 0} J_{\gamma,h'}(\tilde{A}) = J_\gamma(\tilde{A}).$$

Consequently,

$$\lim_{h'\to 0} J_{\gamma,h'}(A_{h'}) = J_\gamma(A) = J_\gamma(\tilde{A}). \tag{3.7}$$

In particular, A is a minimizer of the functional J_γ. Furthermore, direct computation gives

$$\begin{aligned}
&\frac{1}{2}\sum_{\ell=1}^{L} \|A\nabla u^\ell(A) - A_{h'}\nabla u_{h'}^\ell(A_{h'})\|_{L^2(\Omega)^d}^2 + \frac{\gamma}{2}|||A - A_{h'}|||_2^2 \\
&= J_\gamma(A) + J_{\gamma,h'}(A_{h'}) + \sum_{\ell=1}^{L}(A\nabla u^\ell(A) - \vec{h}^\ell, \vec{h}^\ell - A_{h'}\nabla u_{h'}^\ell(A_{h'}))_{L^2(\Omega)^d} - \gamma(A, A_{h'})_{L^2(\Omega)^{d,d}}.
\end{aligned}$$

Now (3.6) and the convergence $A_{h'} \overset{*}{\rightharpoonup} A^0$ in $L^\infty(\Omega)^{d,d}$ imply

$$\lim_{h'\to 0^+}(A\nabla u^\ell(A)-\vec{h}^\ell,\vec{h}^\ell-A_{h'}\nabla u^\ell_{h'}(A_{h'}))_{L^2(\Omega)^d}=\|A\nabla u^\ell(A)-\vec{h}^\ell\|^2_{L^2(\Omega)^d},$$
$$\lim_{h'\to 0^+}(A,A_{h'})_{L^2(\Omega)^{d,d}}=(A,A^0)_{L^2(\Omega)^{d,d}}\geq |||A|||_2^2.$$

These identities together with (3.7) imply

$$\lim_{h'\to 0^+}\frac{1}{2}\sum_{\ell=1}^L\|A\nabla u^\ell(A)-A_{h'}\nabla u^\ell_{h'}(A_{h'})\|^2_{L^2(\Omega)^d}+\frac{\gamma}{2}|||A-A_{h'}|||_2^2$$
$$\leq 2J_\gamma(A)-\sum_{\ell=1}^L\|A\nabla u^\ell(A)-\vec{h}^\ell\|^2_{L^2(\Omega)^d}-\gamma|||A|||_2^2=0,$$

which completes the proof of the theorem. ∎

3.2. Projected Newton algorithm. Based on the necessary optimality system in Theorem 2.12, there are several different ways to develop algorithms for solving the regularized formulation (1.3). One direct choice is gradient descent, which was explored for a related inverse conductivity problem in [15]. Generally, gradient type methods are known to converge steadily but often slowly, especially when the sought-for conductivity tensor is nonsmooth. Thus, it is still of much interest to develop efficient algorithms. In this part we develop a projected Newton algorithm. First we derive the necessary optimal condition of the finite element problem (3.2). The argument in section 2 shows that the directional derivative $J'_{\gamma,h}(A_h)[H]$ of $J_{\gamma,h}(A_h)$ is given by

(3.8)
$$J'_{\gamma,h}(A_h)[H]=\int_\Omega\left(\sum_{\ell=1}^L\nabla u^\ell_h(A_h)\otimes(A_h\nabla u^\ell_h(A_h)-\vec{h}^\ell)+\sum_{\ell=1}^L\nabla u^\ell_h(A_h)\otimes\nabla\bar{p}^\ell_h+\gamma A_h\right)\cdot H dx$$

for any feasible direction $H\in X_h$ such that $A_h+H\in\mathcal{A}_h$, where $u^\ell_h(A_h)=F^\ell_h(A_h)\in V_h$ and $\bar{p}^\ell_h\in V_{h,0}$, $\ell=1,\ldots,L$, solves

$$(A_h\nabla\bar{p}^\ell_h,\nabla v_h)_{L^2(\Omega)^d}+(A_h(A_h\nabla u^\ell_h(A_h)-\vec{h}^\ell),\nabla v_h)_{L^2(\Omega)^d}=0\quad\forall v_h\in V_h(\mathcal{T}). \tag{3.9}$$

The optimality condition can be interpreted pointwise as

$$A_h(x)=P_K\Big(-\frac{1}{\gamma}\Big(\sum_{\ell=1}^L\nabla u^\ell_h(A_h)\otimes(A_h\nabla u^\ell_h-\vec{h})+\sum_{\ell=1}^L\nabla u^\ell_h(A_h)\otimes\nabla\bar{p}^\ell_h\Big)\Big)\quad\text{a.e. in }\Omega. \tag{3.10}$$

In sum, the first-order necessary optimality system in the variational form is given by

$$\begin{cases}(A_h\nabla u^\ell_h,\nabla v_h)_{L^2(\Omega)^d}-(f^\ell,v_h)_{L^2(\Omega)^d}=0\quad\forall v_h\in V_{h,0},\quad\ell=1,\ldots,L,\\ (A_h\nabla\bar{p}^\ell_h,\nabla v_h)_{L^2(\Omega)^d}+(A_h(A_h\nabla u^\ell_h-\vec{h}^\ell),\nabla v_h)_{L^2(\Omega)^d}=0\quad\forall v_h\in V_{h,0},\quad\ell=1,\ldots,L,\\ \Big(\sum_{\ell=1}^L\nabla u^\ell_h\otimes(A_h\nabla u^\ell_h-\vec{h}^\ell)+\nabla u^\ell_h\otimes\nabla\bar{p}^\ell_h+\gamma A_h,D_h-A_h\Big)_{L^2(\Omega)^{d,d}}\geq 0\quad\forall D_h\in\mathcal{A}_h.\end{cases}$$

To apply the Newton method, one crucial step is to derive the Newton update $(\bar{u}^\ell, \bar{p}^\ell, \bar{A})$ for the unknowns (u^ℓ, p^ℓ, A). This can be achieved by solving

$$
\begin{cases}
(\bar{A}\nabla u_h^{\ell,n}, \nabla v_h)_{L^2(\Omega)^d} + (A_h^n \nabla \bar{u}^\ell, \nabla v_h)_{L^2(\Omega)^d} = (A_h^n \nabla u_h^{\ell,n}, \nabla v_h)_{L^2(\Omega)^d} \\
\qquad \forall v_h \in V_{h,0}, \ell = 1, \dots, L, \\
(\bar{A}(\nabla p_h^{\ell,n} + A_h^n \nabla u_h^{\ell,n} - \vec{h}^\ell) + A_h^n(\bar{A}\nabla u_h^{\ell,n}), \nabla v_h)_{L^2(\Omega)^d} + (A_h^n(A_h^n \nabla \bar{u}^\ell, \nabla v_h)_{L^2(\Omega)^d} \\
+ (A_h^n \nabla \bar{p}^\ell, \nabla v_h)_{L^2(\Omega)^d} = (A_h^n \nabla p_h^{\ell,n} + A_h^n(A_h^n \nabla u_h^{\ell,n} - \vec{h}^\ell), \nabla v_h)_{L^2(\Omega)^d} \\
\qquad \forall v_h \in V_{h,0}, \ell = 1, \dots, L, \\
\sum_{\ell=1}^{L} (\nabla u_h^{\ell,n} \otimes (\bar{A}\nabla u_h^{\ell,n}) + \gamma \bar{A} + \nabla \bar{u}^\ell \otimes (A_h^n \nabla u_h^{\ell,n} - \vec{h}^\ell), D_h)_{L^2(\Omega)^{d,d}} \\
+ \sum_{\ell=1}^{L} (\nabla u_h^{\ell,n} \otimes A_h^n \nabla \bar{u}^\ell + \nabla \bar{u}^{\ell,n} \otimes \nabla p_h^{\ell,n} + \nabla \bar{p}^\ell \otimes \nabla u_h^{\ell,n}, D_h)_{L^2(\Omega)^{d,d}} \\
= \sum_{\ell=1}^{L} \left(\nabla u_h^{\ell,n} \otimes (A_h^n \nabla u_h^{\ell,n} - \vec{h}^\ell) + \nabla u_h^{\ell,n} \otimes \nabla p_h^{\ell,n} + \gamma A_h^n, D_h\right)_{L^2(\Omega)^{d,d}} \\
\qquad \forall D_h \in \mathcal{A}_h.
\end{cases} \tag{3.11}
$$

The solution of the coupled system (3.11) is denoted by $\bar{A}_h^n, \bar{u}_h^{\ell,n}, \bar{p}_h^{\ell,n}$, $\ell = 1, \dots, L$. When formulating the Newton method for the KKT system, we do not treat directly the variational inequality (i.e., the box-constraint on the extremal eigenvalues of A_h, or equivalently the projection operator in (3.10)). That is, we use the Newton iteration to update the solution to (3.1), (3.9), and (3.10) without the pointwise projection P_K. After computing the updates, we project the updated solution onto the convex set $\mathcal{A}_h$, which can be performed pointwise. This leads to a projected Newton algorithm, whose details are listed in Algorithm 1. Note that each iteration of the method requires solving one coupled linear system in the state variable $\bar{u}_h^\ell$, adjoint variable $\bar{p}_h^\ell$, and conductivity tensor $\bar{A}_h$. The stopping criterion in line 6 is taken so that the relative error

$$
\max\left\{ \frac{\|\!|A_h^{n+1} - A_h^n|\!\|_2}{\|\!|A_h^{n+1}|\!\|_2}, \frac{\|u_h^{\ell,n+1} - u_h^{\ell,n}\|_{L^2(\Omega)}}{\|u_h^{\ell,n+1}\|_{L^2(\Omega)}}, \frac{\|p_h^{\ell,n+1} - p_h^{\ell,n}\|_{L^2(\Omega)}}{\|\bar{p}_h^{\ell,n+1}\|_{L^2(\Omega)}}, \ell = 1, \dots, L \right\}
$$

falls below a given tolerance τ or the max iteration number exceeds a predetermined number.

It is well known that Newton type algorithms converge very fast, if a good initial guess is provided, which, however, is generally nontrivial. Meanwhile, the choice of the regularization parameter γ is very important in order to obtain satisfactory reconstructions. To choose a suitable regularization parameter and to provide a good initial guess for the Newton algorithm simultaneously, we adopt an easy-to-implement yet very powerful path-following strategy, which has been successfully applied in many applications [29]. Specifically, fix a decreasing factor $\rho \in (0, 1)$, and we apply Algorithm 1 with $\gamma_n = \gamma_0 \rho^n$. with the initial guess given by

Algorithm 3.1 Projected Newton algorithm.

1: Given initial guess $A_h^0, u_h^{\ell,0}, p_h^{\ell,0}$, $\ell = 1, \ldots, L$.
2: **for** $n = 0, 1, 2, \ldots$ **do**
3: Obtain the increments $\bar{A}^n, \bar{u}^{\ell,n}, \bar{p}^{\ell,n}$ of $A_h^n, u_h^{\ell,n}, p_h^{\ell,n}$ by solving the Newton system (3.11).
4: Update $A_h^n, u_h^{\ell,n}, \bar{p}_h^{\ell,n}$ by

$$A_h^{n+1} = A_h^n - \bar{A}_h^n, \quad u_h^{\ell,n+1} = u_h^{\ell,n} - \bar{u}_h^{\ell,n}, \quad p_h^{\ell,n+1} = p_h^{\ell,n} - \bar{p}_h^{\ell,n}, \quad \ell = 1, \ldots, L.$$

5: Project A_h^{n+1} onto $\mathcal{A}_h$, and reset A_h^{n+1}.
6: Check the stopping criterion.
7: **end for**

the solution of the $\gamma_{n-1}-$ problem, i.e.,

$$\min_{A\in\mathcal{A}} \left\{ J_{\gamma_{n-1}}(A) = \frac{1}{2}\sum_{\ell=1}^{L} \|A\nabla u^\ell(A)(f^\ell, g^\ell) - \vec{h}^\ell\|_{L^2(\Omega)^d}^2 + \frac{\gamma_{n-1}}{2}|||A|||_2^2 \right\}.$$

This step warm starts the Newton update and is done to fully exploit the fast local convergence of Newton type methods. The final regularization parameter is determined by the classical discrepancy principle [17, 28], i.e., determining the smallest $k^* \in \mathbb{N}$ such that

$$\sum_{\ell=1}^{L} \|A_{\gamma_{k^*},h}\nabla u_h^\ell(A_{\gamma_{k^*},h})(f^\ell, g^\ell) - \vec{h}^\ell\|_{L^2(\Omega)^d}^2 \le L\delta^2,$$

where $A_{\gamma,h}$ denotes the minimizer for the discrete functional $J_{\gamma,h}$. In summary, there are two loops in the algorithm: one is the inner iteration as shown in Algorithm 3.1, and the other is the outer iteration, which performs the path-following strategy over the penalty parameter γ. Due to the fast local convergence of inner Newton iterations and proper initial guess from the path-following strategy, one often needs only one or two inner iterations to ensure convergence, and hence, Algorithm 3.1 is expected to be highly efficient, which is also confirmed by the extensive numerical experiments in section 4.

4. Numerical experiments and discussions. Now we present several two-dimensional numerical experiments to demonstrate the accuracy and efficiency of the algorithm. All the experiments are carried out using FreeFEM++ [24] on a personal laptop. The domain Ω is taken to be the square $(-1, 1)^2$. We use an $(N + 1) \times (N + 1)$ uniform square grid with $N = 20$ and mesh size $h = 2/N$. The current densities $h^\ell = A\nabla u^\ell$ for reconstructing the conductivity tensor A are simulated by solving problem (1.1) using the Galerkin finite element method with a finer mesh. The noisy data $\vec{h}^{\ell,\delta}$ are generated by perturbing the exact data $\vec{h}^\ell$ pointwise as $\vec{h}^{\ell,\delta}(x) = \vec{h}^\ell(x)(1 + \delta\xi(x))$, where ξ is uniformly distributed on $[-1, 1]$, and $\delta > 0$ denotes the relative noise level. In the numerical experiments, $V_h(\mathcal{T})$ is chosen as P_3 finite element space and $X_h(\mathcal{T})$ is the P_1 discontinuous finite element space. Due to the use of cubic finite elements, the choice $N = 20$ is sufficient for ensuring reasonably accurate reconstructions for noisy data. Numerically this choice is observed to significantly outperform low-order

Table 1

The test cases for the conductivity tensor. The functions $\xi := 2+\sin(\pi x_1)\sin(\pi x_2)$ *and* $\zeta := 0.5\sin(2\pi x_1)$, *and* $l(x) = 1.5\chi_{S_1} + 0.5\chi_{S_2} + 2\chi_{S_3} + \chi_{S_4}$ *with* $S_1 = [-0.4, 0.6] \times [-0.4, 0.6]$, $S_2 = [-1, -0.7] \times [-0.4, 0.1]$, $S_3 = [0.7, 1] \times [-0.8, -0.3]$, *and* $S_4 = \overline{\Omega} \setminus \cup_{i=1}^{3} S_i$.

Example	A_{11}	A_{12}	A_{22}	Feature
1	1	0	1	constant
2	$1+x_1^2+x_2^2$	0	$1+x_1^2+x_2^2$	smooth
3	ξ	0	$1+\zeta^2$	smooth, oscillatory
4	ξ	ζ	$1+x_1^2+x_2^2$	nondiagonal
5	$1+\lvert x_1\rvert+\lvert x_2\rvert$	0	$2+\lvert\sin(\pi x_1)\sin(\pi x_2)\rvert$	nonsmooth
6	$1+\lvert x_1\rvert+\lvert x_2\rvert$	$\lvert x_1x_2\rvert$	$2+\lvert\sin(\pi x_1)\sin(\pi x_2)\rvert$	nonsmooth, nondiagonal
7	$l(x)\xi$	0	$l(x)(1+\zeta^2)$	discontinuous

finite elements. To investigate distinct features of the approach under different problem settings, we consider examples with either diagonal or nondiagonal anisotropic conductivities, and unless otherwise stated, the data correspond to five (i.e., $L = 5$) different Dirichlet data $(g_1, g_2, g_3, g_4, g_5)$, given by $(x_1 + x_2, x_2 + 0.5x_1^2, x_1 - 0.1x_2^2, 0.1(\cos(10x_2) - \cos(10x_1)), x_1x_2)$ and a vanishing source $f \equiv 0$. This choice is motivated by the fact that in the two-dimensional case, four judiciously chosen excitations are sufficient to ensure the unique recovery [8, 7]. The reconstruction procedure is initialized with a constant matrix $A^0 = \left[\begin{smallmatrix} 2 & -1 \\ -1 & 2 \end{smallmatrix}\right]$, and in order to warm start the algorithm, we take $\gamma_0 = 10$ and reduce its value by a factor $\rho = 0.7$ after each inner loop. Below we use $A^\dagger$ (with entries A_{ij}, $i, j = 1, 2$) to denote the exact conductivity tensor. The test cases and their distinct features are listed in Table 1.

The accuracy of a reconstruction $\tilde{A}$ with respect to the exact one $A^\dagger$ is measured by the relative error $e = |||\tilde{A} - A^\dagger|||_2 / |||A^\dagger|||_2$. The relative errors for the examples given in Figures 4.1–4.7 with different noise levels are given in Table 2. It is clearly observed that for all examples, as the noise level δ decreases, the reconstructions become more accurate. For exact data, the reconstruction error e is nonzero, since the mesh used for the inversion step is not very refined, and there is an inevitable discretization error (and also requires suitable regularization). One can also observe that the errors in the reconstruction of the discontinuous conductivity tensor (Example 7) are much larger than the continuous cases in Examples 1–6, since the sharp edges cannot be accurately captured. This clearly indicates the numerical challenge associated with recovering nonsmooth conductivity tensors.

Table 2

The numerical results (accuracy error e) for Examples 1–7.

Example $\setminus\delta$	0%	1%	5%	10%
1	3.490e-4	1.538e-3	4.180e-3	8.456e-3
2	1.492e-3	3.571e-3	8.452e-3	1.237e-2
3	2.731e-3	4.498e-3	1.256e-2	1.963e-2
4	5.496e-3	1.110e-2	2.065e-2	3.249e-2
5	1.771e-3	3.566e-3	9.463e-3	1.438e-2
6	2.499e-3	3.975e-3	9.999e-3	1.509e-2
7	4.970e-2	4.965e-2	5.029e-2	5.283e-2

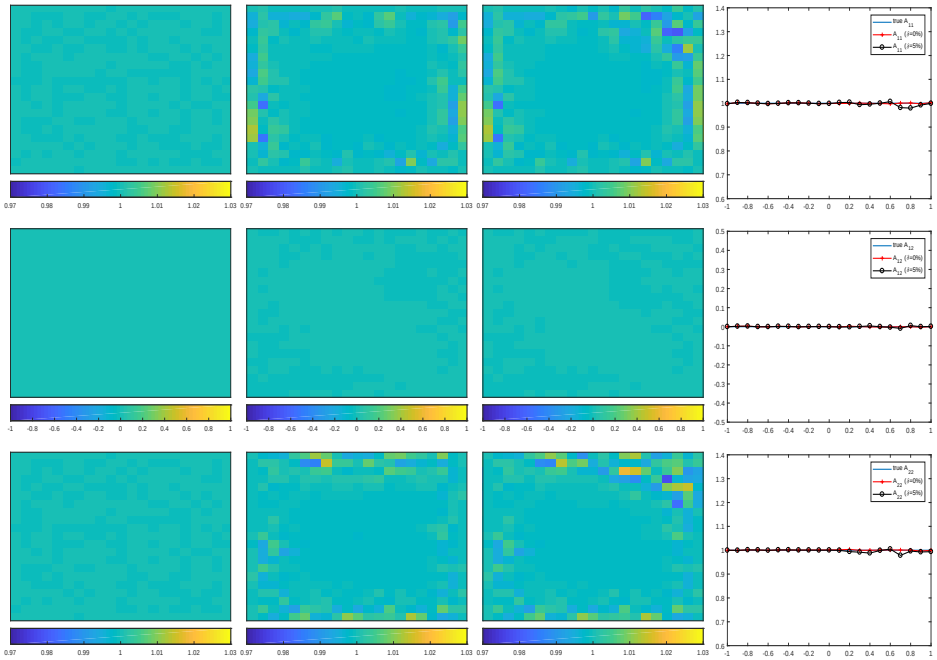

Figure 4.1. *The reconstructions for the conductivity tensor for Example* 1*: the top, middle, and bottom rows refer to* A_{11}*,* A_{12}*, and* A_{22}*, respectively. Column* 1 *is for exact conductivity, column* 2 *for reconstruction with exact data, column* 3 *for noisy data with* $\delta = 5\%$*, and column* 4 *for the cross section along* $\{x_2 = -0.7\}$*.*

To gain further insight into the reconstructions, we present in Figures 4.1–4.7 the exact conductivity tensor, the reconstructed tensors for exact and noisy data, and a cross section. These plots show clearly that the reconstructions are fairly accurate, even in the discontinuous case, agreeing well with the quantitative results in Table 2. Indeed, the kinks in the nonsmooth conductivity components can be accurately resolved, showing clearly the accuracy of the proposed approach. A careful comparison between the results shown in Figures 4.1–4.2 and Figures 4.3–4.7 indicates that the reconstructions of an isotropic conductivity tend to be more stable than the anisotropic case. This is consistent with existing theoretical findings [7, Theorem 2.4]. Nonetheless, Figures 4.5–4.7 show that the approach can also stably and accurately recover an anisotropic conductivity tensor of distinct features for both exact and noisy data (with up to 10% of noise in the data).

Next we briefly examine the convergence behavior of the algorithm. In Figure 4.8, we present the convergence of the relative error and residual for Example 4 versus iteration number (without stopping by the discrepancy principle). It is observed that as the noise level δ decreases from 10% to 0%, the accuracy of the reconstruction $\tilde{A}$ improves steadily, which partly agrees with Theorem 2.14. Also from Figure 4.8, we observe a robust convergence of the algorithm: it converges after about 30 iterations, irrespective of the noise level δ. Although not presented, these observations also hold for other examples. These results confirm the efficiency of the projected Newton algorithm for conductivity tensor recovery.

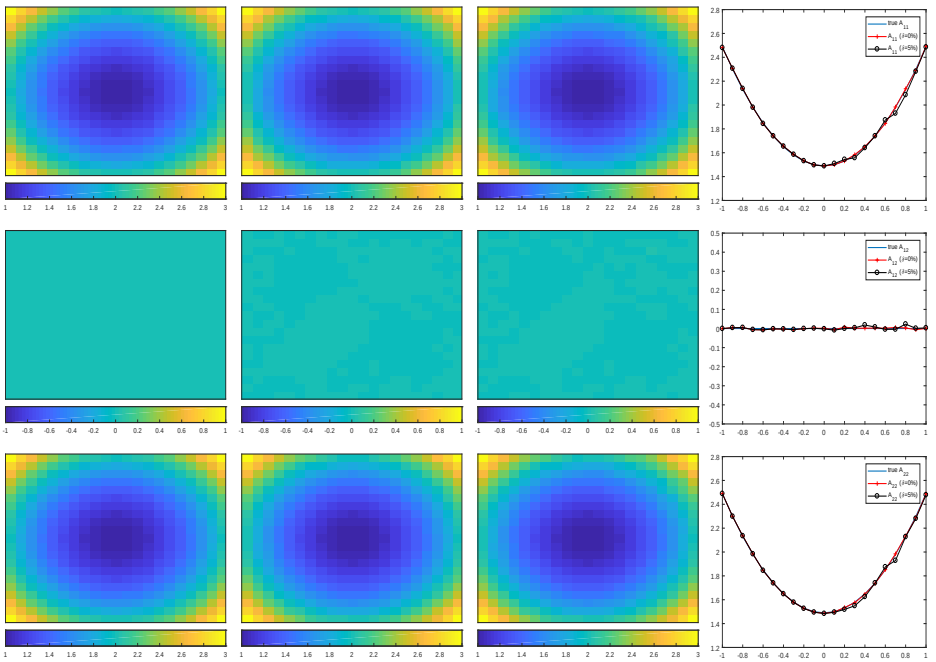

Figure 4.2. *The reconstructions for the conductivity tensor for Example* 2*: the top, middle, and bottom rows refer to* A_{11}*,* A_{12}*, and* A_{22}*, respectively. Column* 1 *is for exact conductivity, column* 2 *for reconstruction with exact data, column* 3 *for noisy data with* $\delta = 5\%$*, and column* 4 *for the cross section along* $\{x_2 = -0.7\}$*.*

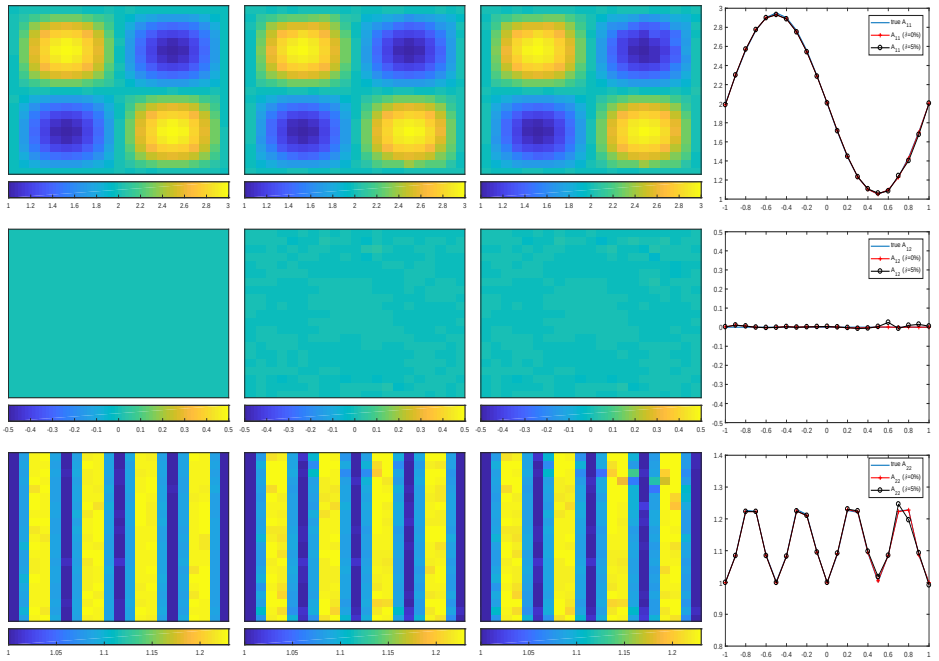

Figure 4.3. *The reconstructions for the conductivity tensor for Example* 3*: the top, middle, and bottom rows refer to* A_{11}*,* A_{12}*, and* A_{22}*, respectively. Column* 1 *is for exact conductivity, column* 2 *for reconstruction with exact data, column* 3 *for noisy data with* $\delta = 5\%$*, and column* 4 *for the cross section along* $\{x_2 = -0.4\}$*.*

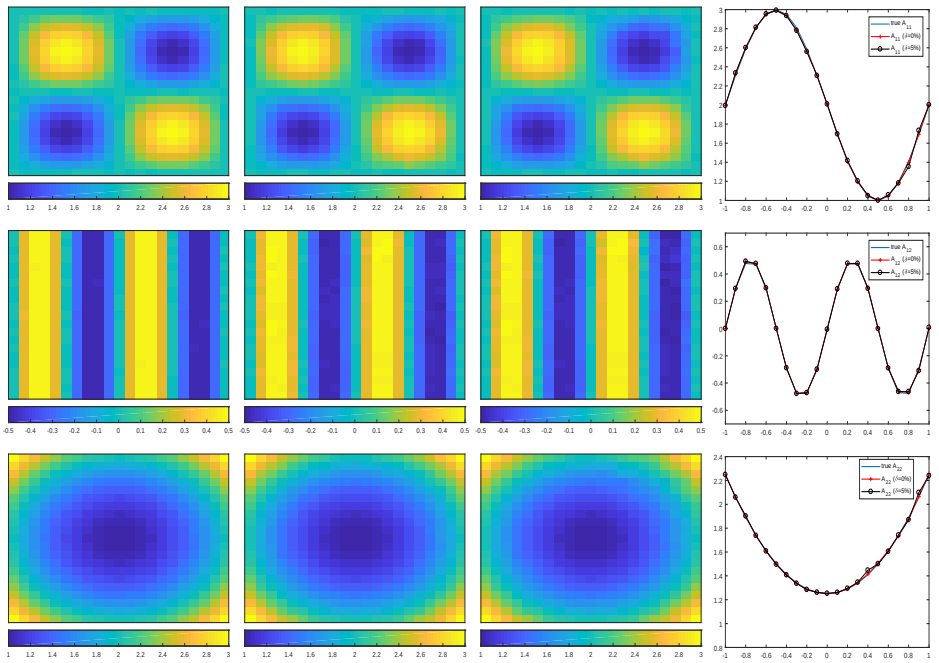

Figure 4.4. *The reconstructions for the conductivity tensor for Example* 4*: the top, middle, and bottom rows refer to* A_{11}*,* A_{12}*, and* A_{22}*, respectively. Column* 1 *is for exact conductivity, column* 2 *for reconstruction with exact data, column* 3 *for noisy data with* $\delta = 5\%$*, and column* 4 *for the cross section along* $\{x_2 = -0.5\}$*.*

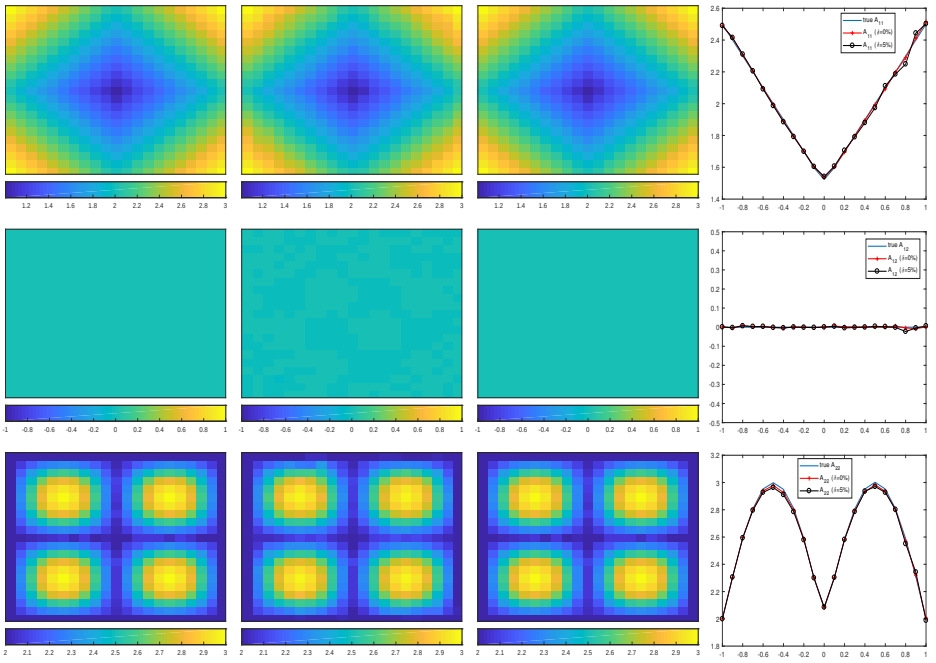

Figure 4.5. *The reconstructions for the conductivity tensor for Example* 5*: the top, middle, and bottom rows refer to* A_{11}*,* A_{12}*, and* A_{22}*, respectively. Column* 1 *is for exact conductivity, column* 2 *for reconstruction with exact data, column* 3 *for noisy data with* $\delta = 5\%$*, and column* 4 *for the cross section along* $\{x_2 = -0.5\}$*.*

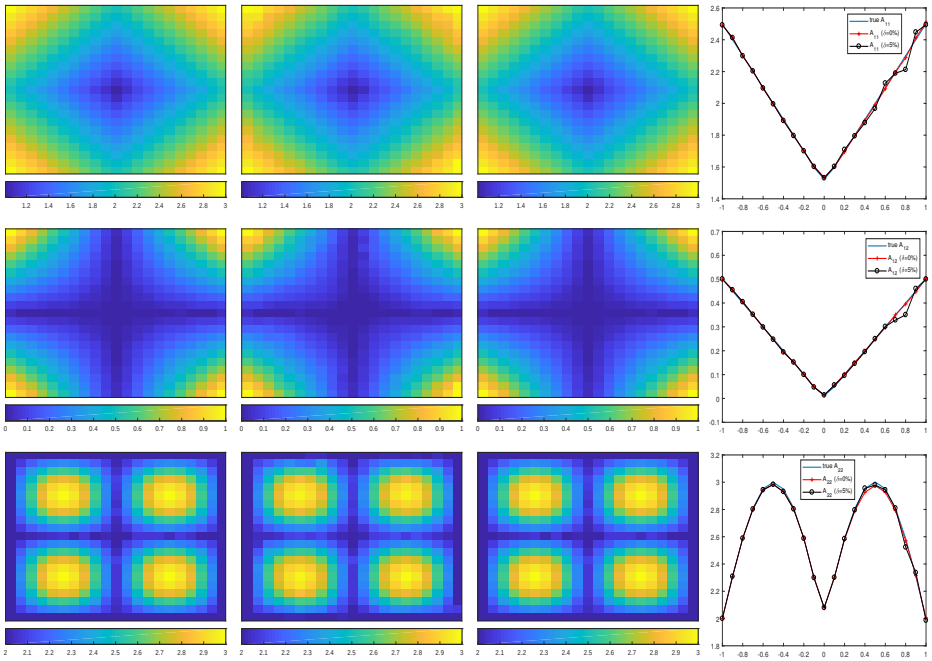

Figure 4.6. *The reconstructions for the conductivity tensor for Example* 6*: the top, middle, and bottom rows refer to* A_{11}*,* A_{12}*, and* A_{22}*, respectively. Column* 1 *is for exact conductivity, column* 2 *for reconstruction with exact data, column* 3 *for noisy data with* $\delta = 5\%$*, and column* 4 *for the cross section along* $\{x_2 = -0.5\}$*.*

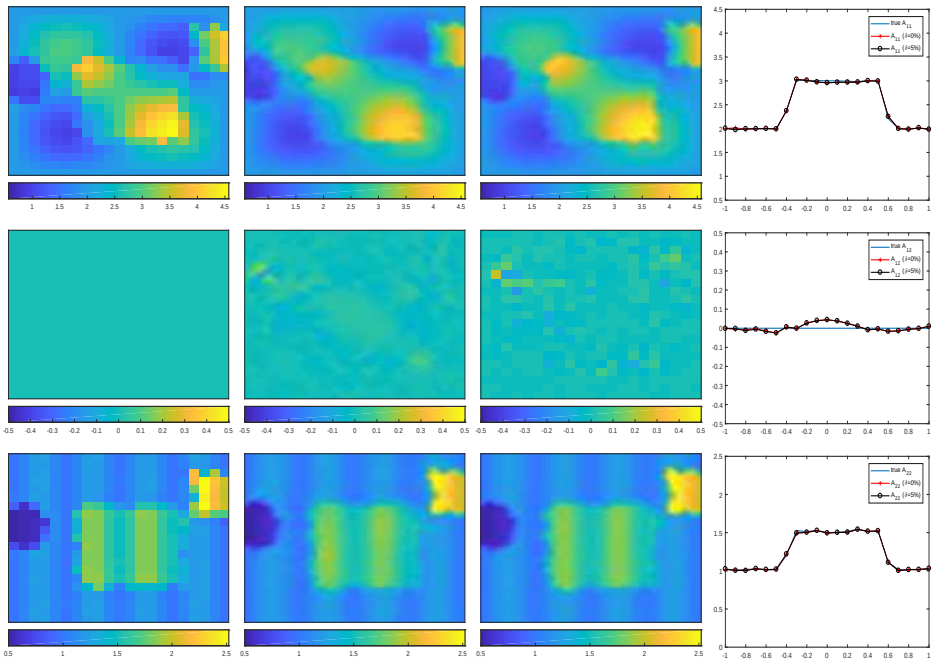

Figure 4.7. *The reconstructions for the conductivity tensor for Example* 7*: the top, middle, and bottom rows refer to* A_{11}*,* A_{12}*, and* A_{22}*, respectively. Column* 1 *is for exact conductivity, column* 2 *for reconstruction with exact data, column* 3 *for noisy data with* $\delta = 5\%$*, and column* 4 *for the cross section along* $\{x_1 = 0\}$*.*

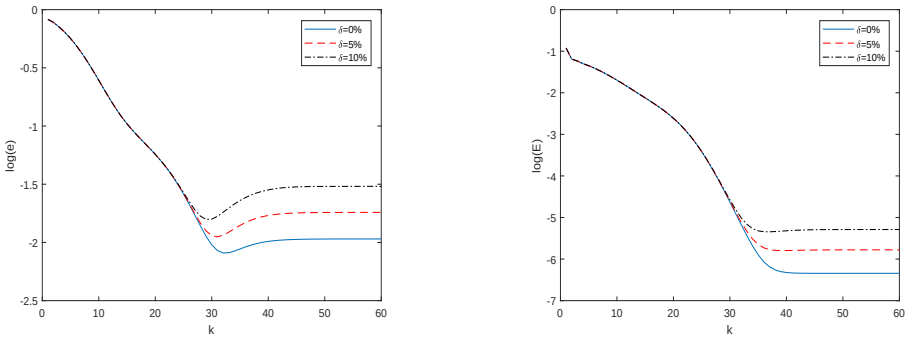

(a) accuracy error e (b) residual E

Figure 4.8. *The convergence of the aglorithm for Example* 4 *with noisy data.*

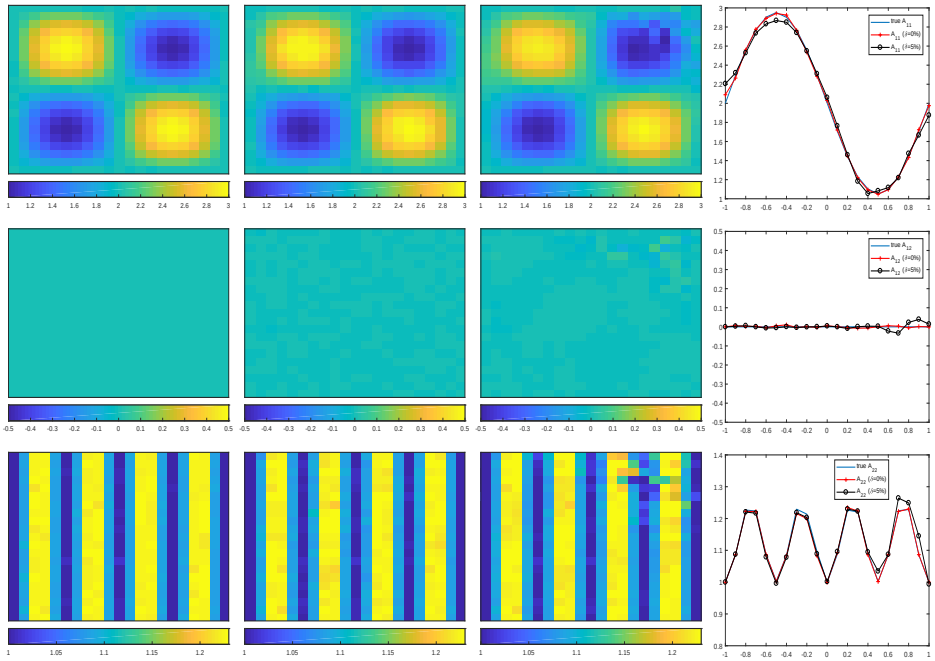

Figure 4.9. *The reconstructions for the conductivity tensor for Example* 3 *with three measurements: the top, middle, and bottom rows refer to* A_{11}, A_{12}, *and* A_{22}, *respectively. Column* 1 *is for exact conductivity, column* 2 *for reconstruction with exact data, column* 3 *for noisy data with* $\delta = 5\%$, *and column* 4 *for the cross section along* $\{x_2 = -0.4\}$.

Last, we examine the influence of the measurement number L on the reconstruction quality. In practice, the number L of available measurements may depend on the specific application. In Figures 4.1–4.7, we have always used five measurements. In Figures 4.9 and 4.10, we repeat Example 3 with three and nine measurements, respectively given by

(i) three Dirichlet inputs $(g^1, g^2, g^3)(x) = (x_1 + x_2, x_2 + 0.5x_1^2, x_1 - 0.1x_2^2)$,

(ii) nine Dirichlet inputs $(g^1, g^2, g^3, g^4, g^5, g^6, g^7, g^8, g^9) = (x_1 + x_2, x_2 + 0.5x_1^2, x_1 - 0.1x_2^2, 0.1(\cos(10x_2) - \cos(10x_1)), x_1x_2, 0.1\sin(10x_1), x_1^2 + x_2^2, x_1 - 0.5x_1^2, 0.1e^{x_1})$.

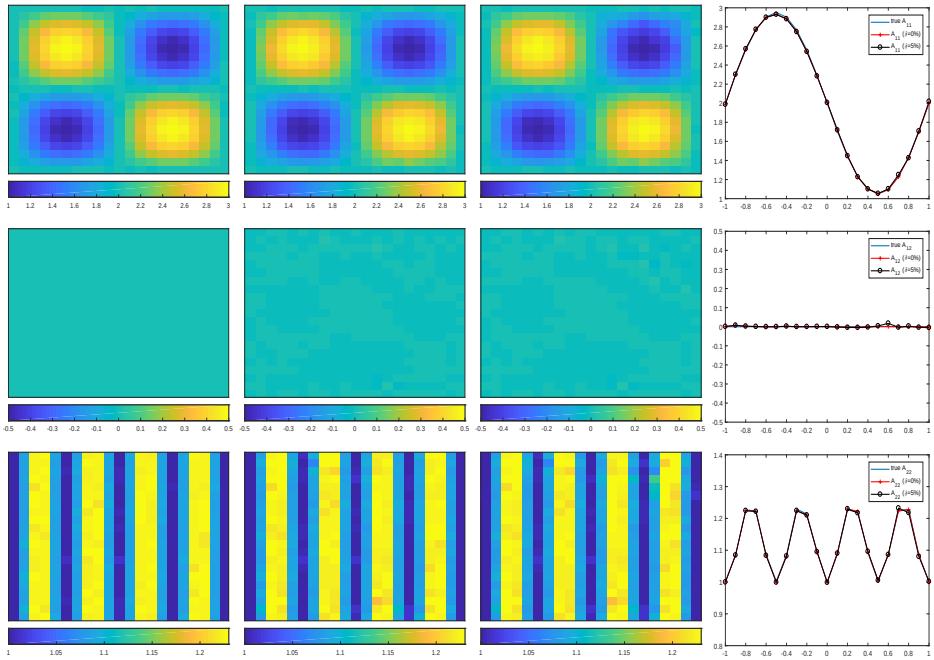

Figure 4.10. *The reconstructions for the conductivity tensor for Example* 3 *with nine measurements: the top, middle, and bottom rows refer to* A_{11}*,* A_{12}*, and* A_{22}*, respectively. Column* 1 *is for exact conductivity, column* 2 *for reconstruction with exact data, column* 3 *for noisy data with* $\delta = 5\%$*, and column* 4 *for the cross section along* $\{x_2 = -0.4\}$*.*

It is observed from Figures 4.3, 4.9, and 4.10 that when the number of measurements increases, the reconstruction becomes more accurate. Thus, a larger number of data is beneficial for recovering conductivity tensors, as one might expect.

5. Conclusions. In this paper, we have studied both analytically and numerically the reconstruction of an anisotropic conductivity tensor A from the knowledge of multiple current densities of the form $A\nabla u$, corresponding to different Dirichlet boundary excitations. We have established important analytical properties, e.g., Lipschitz continuity and Frechét differentiability, of the parameter-to-state map with respect to $L^p(\Omega)^{d,d}$-norms. We proposed and analyzed a regularized formulation of Tikhonov type, which is suitable for both smooth and nonsmooth conductivity tensors. We proved the existence of minimizers and consistency as the noise level tends to zero by means of H-convergence, and derived the necessary optimality system and a Newton algorithm for efficiently solving the coupled system. Also we established the convergence of the finite element approximation by means of Hd-convergence. The extensive numerical simulations clearly showcase the significant potentials of the approach.

Appendix A. Proof of Theorem 2.11.

Proof. Since the penalty is quadratic, its gradient expression and differentiability follow directly. It suffices to compute the gradient of the fidelity term. For any fixed feasible direction H, let $\mathrm{I}_\ell(t) = \frac{1}{2}\|(A+tH)\nabla u^\ell(A+tH) - \vec{h}^\ell\|^2_{L^2(\Omega)^d} - \frac{1}{2}\|A\nabla u^\ell(A) - \vec{h}^\ell\|^2_{L^2(\Omega)^d}$. Clearly,

$$\mathrm{I}_\ell(t) = \tfrac{1}{2}\|(A+tH)\big(\nabla u^\ell(A+tH) - \nabla u^\ell(A)\big) + tH\nabla u^\ell\|_{L^2(\Omega)^d}^2 + \big(A\nabla u^\ell(A) - \vec{h}^\ell, (A+tH)(\nabla u^\ell(A+tH) - \nabla u^\ell(A)) + tH\nabla u^\ell\big)_{L^2(\Omega)^d}.$$

Let $w^\ell = F_\ell'(A)[H]$ be the linearized solution for u^ℓ at A in the direction of H, and let R^ℓ be the corresponding residual, i.e., $R^\ell = u^\ell(A+tH) - u^\ell(A) - tF_\ell'(A)[H]$. Then

$$\mathrm{I}_\ell(t) = \tfrac{t^2}{2}\|(A+tH)(\nabla w^{(i)} + t^{-1}\nabla R^\ell) + H\nabla u^\ell\|_{L^2(\Omega)^d}^2 + \big(A\nabla u^\ell(A) - \vec{h}^\ell, (A+tH)(t\nabla w^\ell + \nabla R^\ell) + tH\nabla u^\ell\big)_{L^2(\Omega)^d}.$$

By the weak formulations for p^ℓ and w^ℓ, we have

$$(A\nabla w^\ell, \nabla p^\ell)_{L^2(\Omega)^d} = -(H\nabla u^\ell, \nabla p^\ell)_{L^2(\Omega)^d},$$
$$(A\nabla p^\ell, \nabla w^{(i)})_{L^2(\Omega)^d} = -(A(A\nabla u^\ell - \vec{h}^\ell), \nabla w^\ell)_{L^2(\Omega)^d}.$$

Subtracting these two identities gives

$$-(H\nabla u^\ell, \nabla p^\ell)_{L^2(\Omega)^d} = -(A(A\nabla u^\ell - \vec{h}^\ell), \nabla w^\ell)_{L^2(\Omega)^d}. \tag{A.1}$$

This and the identity $\|R^\ell\|_{H^1(\Omega)} = O(t^2)$ from the proof of Proposition 2.5 imply

$$\begin{aligned}\lim_{t\to 0^+} t^{-1}\mathrm{I}_\ell(t) &= \lim_{t\to 0^+} \big(A\nabla u^\ell(A) - \vec{h}^\ell, (A+tH)(\nabla w^\ell + t^{-1}\nabla R^\ell) + H\nabla u^\ell\big)_{L^2(\Omega)^d}\\ &= \lim_{t\to 0^+} \big(A\nabla u^\ell(A) - \vec{h}^\ell, tH(\nabla w^\ell + t^{-1}\nabla R^\ell) + H\nabla u^\ell + At^{-1}\nabla R^\ell\big)_{L^2(\Omega)^d}\\ &\quad + (H\nabla u^\ell, \nabla p^\ell)_{L^2(\Omega)^d}\\ &= \big(\nabla u^\ell \otimes \nabla p^\ell + \nabla u^\ell \otimes (A\nabla u^\ell - \vec{h}^\ell), H\big)_{L^2(\Omega)^{d,d}},\end{aligned}$$

which directly gives the expression of $J_\gamma'(A)[H]$. Next, we verify that it defines a bounded linear functional on $L^p(\Omega)^{d\times d}$. For each $\ell = 1, \ldots, L$, it follows from (2.2) that for any $p, q \geq 1$ satisfying $\frac{1}{p} + \frac{1}{q} = \frac{1}{2}$,

$$\begin{aligned}&\big|(\nabla u^\ell \otimes \nabla \bar{p}^\ell + \nabla u^\ell \otimes (A\nabla u^\ell - \vec{h}^\ell), H)_{L^2(\Omega)^{d,d}}\big|\\ &= \big|(H\nabla u^\ell, \nabla \bar{p}^\ell)_{L^2(\Omega)^d} + (H\nabla u^\ell, A\nabla u^\ell - \vec{h}^\ell)_{L^2(\Omega)^d}\big|\\ &\leq |||H|||_p\big(\|\nabla u^\ell\|_{L^q(\Omega)^d}\|\nabla \bar{p}^\ell\|_{L^2(\Omega)^d} + \|\nabla u^\ell\|_{L^q(\Omega)^d}\|A\nabla u^\ell - \vec{h}^\ell\|_{L^2(\Omega)^d}\big)\\ &\leq |||H|||_p\big((\|f^\ell\|_{L^2(\Omega)} + \|g^\ell\|_{H^1(\Gamma)})\|\bar{p}^\ell\|_{H^1(\Omega)} + (\|f^\ell\|_{L^2(\Omega)} + \|g^\ell\|_{H^1(\Gamma)})\|A\nabla u^\ell - \vec{h}^\ell\|_{L^2(\Omega)^d}\big).\end{aligned}$$

Hence, it is a bounded linear functional on $L^p(\Omega)^{d,d}$. Last, we show that it is actually the Fréchet derivative of $J_\gamma(A)$. Let $\mathrm{II}_\ell := \mathrm{I}_\ell(1) - (\nabla u^\ell \otimes \nabla \bar{p}^\ell + \nabla u^\ell \otimes (A\nabla u^\ell - \vec{h}^\ell), H)_{L^2(\Omega)^{d,d}}$. Indeed, we have

$$\mathrm{II}_\ell = \tfrac{1}{2}\|(A+H)\big(\nabla u^\ell(A+H) - \nabla u^\ell(A)\big) + H\nabla u^\ell\|_{L^2(\Omega)^d}^2 + \big(A\nabla u^\ell(A) - \vec{h}^\ell, (A+H)(\nabla u^\ell(A+H) - \nabla u^\ell(A))\big)_{L^2(\Omega)^d} - \big(H\nabla u^\ell, \nabla \bar{p}^\ell\big)_{L^2(\Omega)^d}.$$

This and (A.1) lead to

$$
\begin{aligned}
|\mathrm{II}_\ell| = \Big| & \tfrac{1}{2}\|(A+H)\big(\nabla u^\ell(A+H)-\nabla u^\ell(A)\big)+H\nabla u^\ell\|^2_{L^2(\Omega)^d} \\
& + (A\nabla u^\ell(A)-\vec{h}^\ell, H(\nabla u^\ell(A+H)-\nabla u^\ell(A)))_{L^2(\Omega)^d} + (A\nabla u^\ell(A)-\vec{h}^\ell, A\nabla R)_{L^2(\Omega)^d}\Big| \\
\le\ & \|A+H\|^2_{L^\infty(\Omega)^{d,d}}(\|\nabla u^\ell(A+H)-\nabla u^\ell(A)\|^2_{L^2(\Omega)^d}+\|H\nabla u^\ell\|^2_{L^2(\Omega)^d}) \\
& + \|A\nabla u^\ell(A)-\vec{h}^\ell\|_{L^2(\Omega)^d}\|H\|_{L^\infty(\Omega)^{d,d}}\|\nabla u^\ell(A+H)-\nabla u^\ell(A)\|_{L^2(\Omega)^d} \\
& + \|A\nabla u^\ell(A)-\vec{h}^\ell\|_{L^2(\Omega)^d}\|A\|_{L^\infty(\Omega)^{d,d}}\|\nabla R\|_{L^2(\Omega)^d}.
\end{aligned}
$$

This estimate, Lemma 2.4, and Proposition 2.5 yield the desired differentiability. This completes the proof of the theorem. ∎

Acknowledgment. The authors would like to thank the two anonymous referees for several constructive comments, which have led to an improved presentation.

REFERENCES

[1] B. J. Adesokan, B. Jensen, B. Jin, and K. Knudsen, *Acousto-electric tomography with total variation regularization*, Inverse Problems, 35 (2019), 035008, https://doi.org/10.1088/1361-6420/aaece5.

[2] G. S. Alberti, H. Ammari, B. Jin, J.-K. Seo, and W. Zhang, *The linearized inverse problem in multifrequency electrical impedance tomography*, SIAM J. Imaging Sci., 9 (2016), pp. 1525–1551, https://doi.org/10.1137/16M1061564.

[3] H. Ammari, *An Introduction to Mathematics of Emerging Biomedical Imaging*, Springer, Berlin, 2008.

[4] H. Ammari, S. Boulmier, and P. Millien, *A mathematical and numerical framework for magnetoacoustic tomography with magnetic induction*, J. Differential Equations, 259 (2015), pp. 5379–5405, https://doi.org/10.1016/j.jde.2015.06.040.

[5] H. Ammari, J. Garnier, L. Giovangigli, W. Jing, and J.-K. Seo, *Spectroscopic imaging of a dilute cell suspension*, J. Math. Pures Appl. (9), 105 (2016), pp. 603–661, https://doi.org/10.1016/j.matpur.2015.11.009.

[6] H. Ammari, L. Qiu, F. Santosa, and W. Zhang, *Determining anisotropic conductivity using diffusion tensor imaging data in magneto-acoustic tomography with magnetic induction*, Inverse Problems, 33 (2017), 125006, https://doi.org/10.1088/1361-6420/aa907e.

[7] G. Bal, C. Guo, and F. Monard, *Imaging of anisotropic conductivities from current densities in two dimensions*, SIAM J. Imaging Sci., 7 (2014), pp. 2538–2557, https://doi.org/10.1137/140961754.

[8] G. Bal, C. Guo, and F. Monard, *Inverse anisotropic conductivity from internal current densities*, Inverse Problems, 30 (2014), 025001, https://doi.org/10.1088/0266-5611/30/2/025001.

[9] S. Bartels, C. Carstensen, and G. Dolzmann, *Inhomogeneous Dirichlet conditions in a priori and a posteriori finite element error analysis*, Numer. Math., 99 (2004), pp. 1–24, https://doi.org/10.1007/s00211-004-0548-3.

[10] L. Borcea, *Electrical impedance tomography*, Inverse Problems, 18 (2002), pp. R99–R136, https://doi.org/10.1088/0266-5611/18/6/201.

[11] J. H. Bramble and J. Xu, *Some estimates for a weighted L^2 projection*, Math. Comp., 56 (1991), pp. 463–476, https://doi.org/10.2307/2008391.

[12] S. C. Brenner and L. R. Scott, *The Mathematical Theory of Finite Element Methods*, 3rd ed., Springer, New York, 2008, https://doi.org/10.1007/978-0-387-75934-0.

[13] P. G. Ciarlet, *The Finite Element Method for Elliptic Problems*, North-Holland, Amsterdam, 1978.

[14] K. Deckelnick and M. Hinze, *Identification of matrix parameters in elliptic PDEs*, Control Cybernet., 40 (2011), pp. 957–969.

[15] K. Deckelnick and M. Hinze, *Convergence and error analysis of a numerical method for the identification of matrix parameters in elliptic PDEs*, Inverse Problems, 28 (2012), 115015, https://doi.org/10.1088/0266-5611/28/11/115015.

[16] D. Dos Santos Ferreira, C. E. Kenig, M. Salo, and G. Uhlmann, *Limiting Carleman weights and anisotropic inverse problems*, Invent. Math., 178 (2009), pp. 119–171, https://doi.org/10.1007/s00222-009-0196-4.
[17] H. W. Engl, M. Hanke, and A. Neubauer, *Regularization of Inverse Problems*, Kluwer Academic, Dordrecht, 1996.
[18] L. C. Evans and R. F. Gariepy, *Measure Theory and Fine Properties of Functions*, Stud. Adv. Math., CRC Press, Boca Raton, FL, 1992.
[19] R. Eymard and T. Gallouët, *H-convergence and numerical schemes for elliptic problems*, SIAM J. Numer. Anal., 41 (2003), pp. 539–562, https://doi.org/10.1137/S0036142901397083.
[20] G. J. Fix, M. D. Gunzburger, and J. S. Peterson, *On finite element approximations of problems having inhomogeneous essential boundary conditions*, Comput. Math. Appl., 9 (1983), pp. 687–700, https://doi.org/10.1016/0898-1221(83)90126-8.
[21] K. R. Foster and H. P. Schwan, *Dielectric properties of tissues and biological materials: A critical review*, Crit. Rev. Biomed. Eng., 17 (1989), pp. 25–104.
[22] H. R. Gamba, R. Bayford, and D. Holder, *Measurement of electrical current density distribution in a simple head phantom with magnetic resonance imaging*, Phys. Med. Biol., 44 (1999), pp. 281–91.
[23] S. J. Hamilton, M. Lassas, and S. Siltanen, *A direct reconstruction method for anisotropic electrical impedance tomography*, Inverse Problems, 30 (2014), 075007, https://doi.org/10.1088/0266-5611/30/7/075007.
[24] F. Hecht, *New development in FreeFEM++*, J. Numer. Math., 20 (2012), pp. 251–265, https://doi.org/10.1515/jnum-2012-0013.
[25] N. Hoell, A. Moradifam, and A. Nachman, *Current density impedance imaging of an anisotropic conductivity in a known conformal class*, SIAM J. Math. Anal., 46 (2014), pp. 1820–1842, https://doi.org/10.1137/130911524.
[26] G. C. Hsiao and J. Sprekels, *A stability result for distributed parameter identification in bilinear systems*, Math. Methods Appl. Sci., 10 (1988), pp. 447–456, https://doi.org/10.1002/mma.1670100409.
[27] Y. Ider and L. Muftuler, *Measurement of AC magnetic field distribution using magnetic resonance imaging.*, IEEE Trans. Med. Imaging, 16 (1997), pp. 617–622.
[28] K. Ito and B. Jin, *Inverse Problems: Tikhonov Theory and Algorithms*, World Scientific, Hackensack, NJ, 2015.
[29] Y. Jiao, B. Jin, and X. Lu, *A primal dual active set with continuation algorithm for the ℓ^0-regularized optimization problem*, Appl. Comput. Harmon. Anal., 39 (2015), pp. 400–426, https://doi.org/10.1016/j.acha.2014.10.001.
[30] M. Joy, G. Scott, and M. Henkelman, *In vivo detection of applied electric currents by magnetic resonance imaging*, Magn. Reson. Imaging, 7 (1989), pp. 89–94, https://doi.org/10.1016/0730-725X(89)90328-7.
[31] C. E. Kenig, M. Salo, and G. Uhlmann, *Reconstructions from boundary measurements on admissible manifolds*, Inverse Probl. Imaging, 5 (2011), pp. 859–877, https://doi.org/10.3934/ipi.2011.5.859.
[32] M.-S. Ko and Y.-J. Kim, *Resistivity tensor imaging via network discretization of Faraday's law*, SIAM J. Imaging Sci., 10 (2017), pp. 1–25, https://doi.org/10.1137/16M1074643.
[33] R. V. Kohn and B. D. Lowe, *A variational method for parameter identification*, RAIRO Modél. Math. Anal. Numér., 22 (1988), pp. 119–158, https://doi.org/10.1051/m2an/1988220101191.
[34] O. Kwon, J.-Y. Lee, and J.-R. Yoon, *Equipotential line method for magnetic resonance electrical impedance tomography*, Inverse Problems, 18 (2002), pp. 1089–1100, https://doi.org/10.1088/0266-5611/18/4/310.
[35] O. Kwon, E. Woo, J. Yoon, and J. Seo, *Magnetic resonance electrical impedance tomography (MREIT): Simulation study of J-substitution algorithm*, IEEE Trans. Biomed. Eng., 49 (2002), pp. 160–167.
[36] N. G. Meyers, *An L^p-estimate for the gradient of solutions of second order elliptic divergence equations*, Ann. Sc. Norm. Super. Pisa Cl. Sci. (3), 17 (1963), pp. 189–206.
[37] F. Monard and G. Bal, *Inverse anisotropic diffusion from power density measurements in two dimensions*, Inverse Problems, 28 (2012), 084001, https://doi.org/10.1088/0266-5611/28/8/084001.
[38] F. Monard and G. Bal, *Inverse anisotropic conductivity from power densities in dimension $n \geq 3$*, Comm. Partial Differential Equations, 38 (2013), pp. 1183–1207, https://doi.org/10.1080/03605302.2013.787089.

[39] F. Monard and D. Rim, *Imaging of isotropic and anisotropic conductivites from power densities in three dimensions*, Inverse Problems, 34 (2018), pp. 075005, https://doi.org/10.1088/1361-6420/aabe5a.
[40] T. Morimoto, S. Kimura, Y. Konishi, K. Komaki, T. Uyama, Y. Monden, D. Y. Kinouchi, and D. T. Iritani, *A study of the electrical bio-impedance of tumors*, Invest. Surg., 6 (1993), pp. 25–32.
[41] F. Murat and L. Tartar, *H-Convergence*, Progr. Nonlinear Differential Equations Appl. 31, Birkhäuser Boston, Boston, MA, 1997.
[42] A. Nachman, A. Tamasan, and A. Timonov, *Conductivity imaging with a single measurement of boundary and interior data*, Inverse Problems, 23 (2007), pp. 2551–2563, https://doi.org/10.1088/0266-5611/23/6/017.
[43] A. Nachman, A. Tamasan, and A. Timonov, *Recovering the conductivity from a single measurement of interior data*, Inverse Problems, 25 (2009), 035014, https://doi.org/10.1088/0266-5611/25/3/035014.
[44] P. W. Nicholson, *Specific impedance of cerebral white matter*, Exp. Neurol., 13 (1965), pp. 386–401, https://doi.org/10.1016/0014-4886(65)90126-3.
[45] B. J. Roth, *The Electrical Conductivity of Tissues*, in The Biomedical Engineering Handbook, CRC Press, Boca Raton, FL, 2000, pp. 10.1–10.12.
[46] S. Rush and D. Driscoll, *Current distribution in the brain from surface electrodes*, Anesth. Analg., 47 (1968), pp. 717–723.
[47] G. Scott, M. Joy, R. Armstrong, and R. Henkelman, *Measurement of nonuniform current density by magnetic resonance*, IEEE Trans. Med. Imag., 10 (1991), pp. 362–374, https://doi.org/10.1109/42.97586.
[48] J. K. Seo, H. C. Pyo, C. Park, O. Kwon, and E. J. Woo, *Image reconstruction of anisotropic conductivity tensor distribution in MREIT: Computer simulation study*, Phys. Med. Biol., 49 (2004), pp. 4371–4382, https://doi.org/10.1088/0031-9155/49/18/012.
[49] J. K. Seo and E. J. Woo, *Magnetic resonance electrical impedance tomography (MREIT)*, SIAM Rev., 53 (2011), pp. 40–68, https://doi.org/10.1137/080742932.
[50] G. Strang and G. Fix, *An Analysis of the Finite Element Method*, Prentice-Hall, Englewood Cliffs, NJ, 1973.
[51] L. Tartar, *The General Theory of Homogenization, A Personalized Introduction*, Springer-Verlag, Berlin, 2009, https://doi.org/10.1007/978-3-642-05195-1.
[52] G. Uhlmann, *Electrical impedance tomography and Calderón's problem*, Inverse Problems, 25 (2009), 123011, https://doi.org/10.1088/0266-5611/25/12/123011.
[53] T. Widlak and O. Scherzer, *Hybrid tomography for conductivity imaging*, Inverse Problems, 28 (2012), 084008, https://doi.org/10.1088/0266-5611/28/8/084008.
[54] H. Yazdanian and K. Knudsen, *Numerical conductivity reconstruction from partial interior current density information in three dimensions*, Inverse Problems, 37 (2021), 105010, https://doi.org/10.1088/1361-6420/ac1e81.